PROJEKTNR. 14006

Förbättring av träaskors puzzolana aktivitet i ekologisk betong – del 1

Slutrapport

Ece Teker

2023-08-17

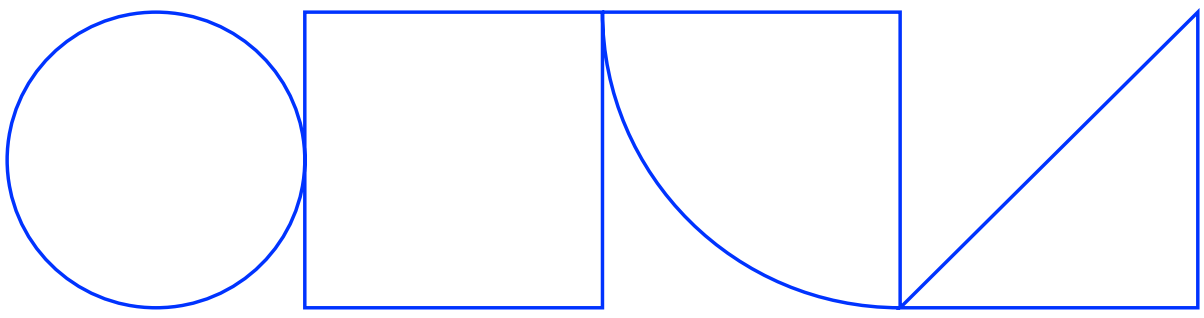

MID-TERM REPORT

Use of Wood Ash in Ecological Concrete

Ece Ezgi Teker Ercan

Building Materials

LULEÅ TEKNISKA UNIVERSITET

LULEÅ TEKNISKA UNIVERSITET

Use of Wood Ash in Ecological Concrete

by

Ece Ezgi Teker Ercan

Mid-Term Report

Luleå, August 2023

Building Materials
Department of Civil, Environmental and Natural Resources Engineering
Luleå University of Technology
SE-97187 Luleå, Sweden

ACKNOWLEDGEMENTS

This midterm report has been prepared in the Building Materials group, Department of Civil, Environmental and Natural Resources Engineering, Luleå University of Technology, Sweden. This research was founded by the Development Fund of the Swedish Construction Industry (SBUF), Skanska and LTU Createrity. I would like to thank to Stenvalls Trä AB for providing the wood ash that was used in this project.

I would like to express my deepest gratitude:

To my supervisor, Assoc. Prof. Karin Habermehl-Cwirzen, for her precious guidance and support.

To my co-supervisor Assoc. Prof. Lale Andreas, and Prof. Andrzej Cwirzen, for their valuable comments and advice.

To my colleagues in the Building Materials group, for their friendship and helpful suggestions. A special thanks to Carina Hannu for her administrative guidance.

Last but not least, to my family – my parents and brother Bartu – for their unconditional love and unwavering support. Without them, none of this would have been possible. I am also deeply thankful to my husband, Umut, for his love, patience, and companionship in Luleå, and to our lovely cat Nobilis for his comforting presence.

Ece Ezgi Teker Ercan

Luleå, August 2023

SUMMARY

Cement production contributes significantly to carbon dioxide emissions, prompting the exploration of eco-friendly binders to mitigate its environmental impact. Wood ash has emerged as a promising alternative, primarily sourced from power plants. Although higher wood ash content in concrete and mortars can negatively affect strength and durability, it still holds potential as as an alternative binder. Depending on the chemical composition wood ash and the replacement ratio of cement with it can even lead to slight improvements in the strength and durability of concrete, with the optimal replacement level ranging from 10% to 20%. However, more extensive research is necessary to fully comprehend the impact of wood ash on cement-based materials' durability and their suitability for alkali-activated materials.

This study aims to investigate the reactivity of wood ash ground using a planetary ball mill, as well as to examine the resulting material's mechanical properties. The pozzolanic reactivity of wood ash was determined by comparing various grinding durations with untreated wood ash, using a 20 wt% replacement for Portland cement in the Frattini Test and assessing the Strength Activity Index (SAI). Preliminary results indicate that grinding the wood ash enhances its pozzolanic activity.

Furthermore, the research explored the effects of using ground wood ash as a partial replacement for ground granulated blast furnace slag at 10 wt% and 20 wt% in alkali-activated mortars. The study involved three different alkali activators: sodium silicate (Na_2SiO_3), sodium carbonate (Na_2CO_3), and sodium hydroxide (NaOH). The main objective was to evaluate how different grinding times of wood ash affected the mechanical properties of the alkali-activated mortars when combined with various alkali activators. The results revealed that grinding improves the mechanical strength of mortars containing wood ash. However, increasing the wood ash ratio led to reduced mechanical strength and increased porosity.

Overall, the findings suggest that grinding wood ash enhances its pozzolanic activity, making it a promising eco-friendly replacement for cement. Moreover, exploring its use as a partial ground granulated blast furnace slag replacement in alkali-activated mortars with different activators offers possibilities for sustainable construction practices with improved mechanical properties. Nevertheless, further research is needed to fully comprehend and optimize the potential of wood ash in these applications.

SAMMANFATTING

Cementproduktion bidrar avsevärt till koldioxidutsläppen, vilket föranleder forskning kring miljövänliga bindemedel för att mildra dess miljöpåverkan. Träaska kan vara ett lovande alternativ, främst från kraftverk där trä är det dominerande bränslet. Även om högre halter av träaska i betong och murbruk kan påverka styrka och hållbarhet negativt, har det fortfarande potential som alternativt bindemedel. Beroende på den kemiska sammansättningen av träaska och ersättningsförhållandet för cement med den kan till och med leda till små förbättringar av betongens hållfasthet och hållbarhet, med den optimala ersättningsnivån från 10 % till 20 %. Mer omfattande forskning krävs dock för att fullt ut förstå träaskans inverkan på cementbaserade materialens hållbarhet och deras lämplighet för alkaliaktiverade material.

Denna studie syftar till att undersöka reaktiviteten hos träaska som mals med hjälp av en planetkulkvarn, samt att undersöka det resulterande materialets mekaniska egenskaper. Puzzolanreaktiviteten hos träaska bestämdes genom att jämföra olika malningstider med obehandlad träaska, med användning av en 20 viktprocent ersättning för Portlandcement i Frattini-testet och bedömning av Strength Activity Index (SAI). Preliminära resultat tyder på att slipning av träaskan ökar dess puzzolanaktivitet.

Dessutom undersöktes effekterna av att använda mald träaska som partiell ersättning för mald granulerad masugnsslagg vid 10 viktprocent och 20 viktprocent i alkaliaktiverade murbruk. Studien involverade tre olika alkaliaktivatorer: natriumsilikat (Na_2SiO_3), natriumkarbonat (Na_2CO_3) och natriumhydroxid (NaOH). Huvudsyftet var att utvärdera hur olika maltider av träaskan påverkade de alkaliaktiverade brukens mekaniska egenskaper i kombination med olika alkaliaktivatorer. Resultaten visade att malningförbättrar den mekaniska hållfastheten hos bruk som innehåller träaska. En ökning av andelen träaska ledde dock till minskad mekanisk hållfasthet och ökad porositet.

Sammantaget tyder resultaten på att malning av träaska ökar dess puzzolanaktivitet, vilket gör den till en lovande miljövänlig ersättning för cement. Att utforska dess användning som en partiell slaggersättning i alkaliaktiverade murbruk med olika aktivatorer erbjuder dessutom möjligheter till hållbara byggmetoder med förbättrade mekaniska egenskaper. Ändå behövs ytterligare forskning för att fullt ut förstå och optimera potentialen hos träaska i dessa applikationer.

TABLE OF CONTENTS

TERMS AND ABBREVIATIONS

Abbreviations	Description
ASR	Alkali-silica reaction
B/P	Ball to powder ratio
C-S-H	Calcium aluminum silicate hydrate
C-A-S-H	Calcium silicate hydrate
FA	Fly ash
GGBFS	Ground Granulated Blast Furnace Slag
HM	Hydration modulus
Kb	Basicity coefficient
LOI	Loss on ignition
N-A-S-H	Sodium aluminum silicate hydrate
Ms	Alkali modulus
PC	Portland cement
rpm	Round per minute
SAI	Strength Activity Index
SEM	Scanning Electron Microscopy
SC	Sodium carbonate
SH	Sodium hydroxide
SS	Sodium silicate
s/b	Sand to binder ratio
WFA1	Wood fly ash 1
WFA2	Wood fly ash 2
WFA3	Wood fly ash 3
WFA3-0	Sieved wood fly ash 3
WFA3-10	Sieved wood fly ash 3 (ground for 10 min)
WFA3-20	Sieved wood fly ash 3 (ground for 20 min)
WA	Wood Ash
WA10	Wood Ash (10 min ground)
WA20	Wood Ash (20 min ground)
w/b	Water to binder ratio
XRD	X-ray Diffractometer

LIST OF FIGURES

LIST OF TABLES

1. Introduction

Concrete is widely utilized in the construction industry due to its good mechanical properties, durability, and affordability [1,2]. However, Portland cement, which is the main component of concrete, contributes significantly to carbon dioxide emissions due to the composition of clinker produced by burning limestone in cement plants. This chemical process, referred to as calcination, involves the decomposition of calcium carbonate ($CaCO_3$) into calcium oxide (CaO) and carbon dioxide (CO_2), leading to substantial emissions of greenhouse gases [3–5]. The production of Portland cement emits between 500 and 900 kg of CO_2 per ton of cement and is responsible for about 5–8% of global carbon dioxide emissions [6–8]. In 2020, the Global Cement and Concrete Association [9] reported a global production of approximately 14 billion cubic meters of concrete and 4.2 billion tons of cement.

It is crucial to enhance the use of supplementary cementitious materials for creating sustainable concrete to address the environmental impacts associated with cement manufacturing. There is a growing demand for solutions that reduce CO_2 emissions and utilize waste materials, in line with the goals of the Paris Agreement, which emphasizes the urgency of preventing global temperatures from rising above 1.5°C [10]. Fly ash, an industrial by-product has been successfully utilized as cement replacement and produces more durable and cost-effective construction materials. However, the availability of fly ash is declining due to the closure of coal-based thermal power plants worldwide [11]. As an alternative, biomass and wood ash emerge as sustainable options to replace fly ash [12,13].

Wood ash is composed of both organic and inorganic content resulting from the combustion of wood and wood products. When wood is burned, about 6-10% of its weight is transformed into ash [14]. Globally, the production of woody biomass amounts to approximately 4600 million tons each year, with 60% used for energy generation, 20% for industrial purposes, and the remaining 20% lost during primary production and decomposition in the field [15]. Currently, a significant portion of wood ash is discarded in landfills, while some are employed in agriculture and forestry [16,17]. However, there are concerns surrounding these applications of wood ash. One concern is the expected increase in costs due to future challenges in finding suitable landfill areas [5,18]. Moreover, landfilling of wood ash can lead to the release of hazardous elements, potentially contaminating groundwater [19]. Health risks may also arise from the airborne dispersion of fine particles by wind during wood ash landfilling [20,21]. The use of certain agricultural practices involving wood ash may also pose risks due to the presence of heavy metal content

and acidic pH levels [22]. As an alternative, utilizing wood ash in concrete appears to be a more sustainable option compared to other disposal methods [14].

Compared to coal fly ash, the quality control of wood ash is more challenging. This difficulty arises from the variations in the organic and inorganic composition of wood ash, influenced by factors such as tree species, tree parts, geographical location of the tree's growth, combustion technology and temperature, collection method from the boiler, and storage conditions [4,16,23,24]. It is worth noting that while conventional fly ash in concrete aligns with standards like EN 450-1 [25] and ASTM C 618 [26], wood ash usage in concrete does not currently comply with these standards. Nevertheless, previous scientific research demonstrates that wood ash can still find applications in the construction industry, despite not meeting all standard usage recommendations [19,20,23,27–30].

1.1. Aim, scope and limitations

The primary objective of this project was to explore the potential of using wood ash in both alkali-activated and cement-based materials for the development of ecological building materials, with a focus on reducing the high CO_2 emissions associated with Portland cement production. The research started with an extensive literature review to investigate the existing knowledge and previous studies on the use of wood ash in alkali-activated and cement-based materials.

The experimental part, initially focused on the use of wood ash as a precursor in alkali-activated mortars activated with sodium silicate. The project has involved conducting preliminary tests to optimize the ball milling parameters for the wood ash and subsequently conducting different trials to determine its impact on the properties of alkali-activated mortars.

Another essential aspect of this study involved examining the pozzolanic properties of wood ash by using it as a cement replacement. By assessing its behaviour as a partial substitute for cement, this research aimed to identify the potential benefits and drawbacks of using wood ash in cement-based materials.

Furthermore, this project investigated the utilization of wood ash as a replacement for ground granulated blast furnace slag in alkali-activated systems that employ different alkali activators. This investigation seeks to evaluate the influence of wood ash in combination with different alkali activators on the mechanical and microstructural properties of alkali-activated materials.

The experimental works have been so far conducted only on a small scale, and while they provide valuable insights, the findings may not fully represent the

complexities of large-scale industrial applications. Moreover, this study primarily focused on preliminary tests, and more in-depth research will be necessary to fully understand the long-term durability and environmental impacts of wood ash-based construction materials for the second half of the project.

1.2. Research questions

The following research questions were formulated for the project:

1. How does the different wood ash grinding parameters affected alkali-activated wood ash? **(Study A)**
2. How does the pozzolanic activity of wood ash is affected by ball milling? **(Study C)**
3. How do different types of alkali-activators affect the mechanical properties of wood ash-containing alkali-activated mortars? **(Study D – Paper II)**
4. How does the chemical composition of wood ash affect the properties of concrete?
5. How the effect of variability of properties of wood ashes originating from different sources on their reactivity (used as SCM and as precursor in alkali activated system) could be limited?

1.3. Chapter overview

The report is included of six chapters which are briefly described below:

Chapter 1 introduces the aim, scope, limitation, and research questions.

Chapter 2 presents literature review.

Chapter 3 describes the materials and methods used in this project.

Chapter 4 presents the results and discussions of the conducted test and analysis.

Chapter 5 summarizes the conclusion of the study.

Chapter 6 presents further research for the second part of the PhD project.

1.4. List of appended publications

The following publications are included in this mid-term report.

Paper I — Teker Ercan, E.E.; Andreas, L.; Cwirzen, A.; Habermehl-Cwirzen, K. Wood Ash as Sustainable Alternative Raw Material for the Production of Concrete—A Review. Materials. 2023, 16, 2557, doi:10.3390/ma16072557.

Paper II — Teker Ercan, E.E.; Cwirzen, A.; Habermehl-Cwirzen, K. The Effects of Partial Replacement of Ground Granulated Blast Furnace Slag by Ground Wood Ash on Alkali-Activated Binder Systems. Materials. 2023, 16, 5347.

2. Literature review

This chapter provides an overview of use of wood ash as a cement replacement in traditional concrete and use of it in alkali-activated systems.

2.1. Characteristics of wood ash

Many studies have shown that wood ash particles have a porous structure [6, 24, 30, 32]. Compared to Portland cement, wood ash has larger and more irregular particles, resulting in larger specific surface areas [30, 34–37]. Also, wood fly ash particles have higher surface porosity and are more angular than coal fly ash particles. Particle size and surface area are crucial factors influencing setting and water demand [33], with finer particles positively affecting the reactivity [32]. Wood ash has a lower density compared to Portland cement resulting in a significant reduction in unit weight when used as a cement replacement [23]. Carević et al. [32] observed that wood bottom ash particles are coarser compared to wood fly ash and cement particles.

The chemical composition of wood ash can vary depending on combustion temperature and methods, as well as the type of wood used [31]. Wood ash has high alkalinity, which might cause delayed concrete setting and potential durability issues due to alkali-aggregate reactions [28,32]. It contains high levels of SO_3, which could lead to sulfate attack and concrete deterioration [20,28,32]. Washing treatment was successfully used to remove sulfates, alkalis, chlorides and soluble compounds from wood ash [23,33].

Many studies reported that major components of wood ash are lime, calcite, portlandite, calcium silicate, and silicates [16,34]. Wood ash can be used as a cement replacement (SCM) due to its amorphous silica content [35]. Additionally, crystalline phases like calcite, gypsum, anhydrite, quartz, tridymite, magnetite, hematite, rutile, and muscovite have been detected in wood ash [29,35]. The presence of wood ash in cement pastes can affect the formed phases, with increasing wood ash content influencing the intensity of calcium silicate and ettringite peaks [29]. Wood ash has also been found to contain SiO_2 in both amorphous and crystalline forms [36].

Loss on Ignition (LOI) indicates the presence of unburnt organic content due to incomplete or uncontrolled incineration and it might vary based on the analysis temperature [27–29]. The standard testing methods ASTM C311 [37] and EN 196-2 [38] prescribe different temperatures for determining LOI: 750 ± 50 °C and 950 ± 25 °C, respectively. The maximum allowable limits for LOI in ASTM C618 [26] vary depending on the type of fly ash, ranging from 6% to 10%, while EN 450-1 [25]

specifies limits between 5% and 9%. High LOI values in wood ash can negatively impact pozzolanic and durability properties, workability, setting, and mechanical strength of concrete, as well as the effectiveness of chemical admixtures [23,28,39]. Various methods have been proposed to reduce the unburnt carbon content in wood ash, such as sieving, re-calcining treatment, grinding, and water-washing treatments, which can improve the properties of wood ash when used as supplementary cementitious material in concrete [23,40,41].

Pozzolanic activity is the result of a reaction between calcium hydroxide and alumina silicates, creating a binding hydration product [42]. The pozzolanic property is determined by the sum of pozzolanic oxides (SiO_2, Fe_2O_3, and Al_2O_3), which should be above 70% according to EN 450-1 [25]. Pozzolanic oxides of wood ash vary ranging from 13.03% [43] to 88.32% [6], according to the literature. Many studies confirm the pozzolanic behaviour of wood ash [6,29,34,36,44], although some studies report no pozzolanic activity due to low SiO_2 content and high LOI [30,45].

Hydraulic binders are materials that form hydration products through reactions with water and can harden and maintain strength even underwater [20,43,46]. Hydraulic activity relies on the SiO_2 and CaO content, with a required CaO to SiO_2 ratio greater than 2 according to EN 197-1 [47]. Due to its high CaO content, wood ash might also exhibit hydraulic behaviour [48]. Some studies attribute increased compressive strength to hydraulic properties rather than pozzolanic activity [23].

2.2. Use of wood ash as cement replacement in mortar and concrete

2.2.1. Fresh properties

Researchers generally agree that increasing the wood ash ratio in blended cement leads to a decreased workability of the concrete [4,19,23,39,49,50]. The reduction in workability is attributed to factors such as the irregular shape and higher specific surface area of porous wood fly ash particles, which differ from those of Portland cement particles [23]. Additionally, higher LOI values of wood fly ash have been associated with decreased workability, although water-washing treatment can improve it [23]. However, some studies have reported no significant influence on workability with low wood ash replacement ratios [51,52], while higher replacement ratios tend to decrease it [49,53]. The presence of unburnt carbon in wood ash absorbing water can further contribute to reduced workability in higher replacement ratios [53].

Numerous research studies have confirmed that incorporating wood ash into cement-based materials generally leads to a delay in setting times. This delay becomes more pronounced as the proportion of wood ash used as a replacement for cement increases [23,27,32,39,53,54]. Various factors contribute to the delayed setting, including high levels of alkali and magnesium oxide in the wood ash [32], a high LOI [55], and the concentration of C_3A [53]. On the other hand, when lower amounts of wood ash are used (e.g., 10 wt%), the setting process can actually be accelerated due to the alkalis in the ash dissolving cement ions [53]. The mineral composition of the wood ash, the formation of carboaluminates and carbonates during cement hydration, and the impact of the fine particle size of wood ash on the workability of the cement paste also play a role in influencing the setting times [56]. Additionally, studies have shown that with higher wood ash contents, particularly at 20 wt% and 30 wt%, the setting times can become shorter due to increased water consumption caused by the presence of organic matter in the ash [29].

2.2.2. Mechanical properties

Wood ash as a cement replacement in concrete typically leads to decreased compressive strength [19,54], with some exceptions [29]. Higher wood ash ratios are generally associated with reduced compressive strength, although certain cases show slight improvements with specific ash ratios [57]. Moreover, compressive strength improvement might be observed in later ages [30]. The primary factors responsible for the reduction in early-age strength were the higher wood ash ratio, increased free CaO, and high alkali content [32].

Similarly, the split tensile strength of concrete follows similar trends as the compressive strength when using wood ash as a cement replacement. Overall, an increase in wood ash ratio tends to reduce the split tensile strength [17,58,59]. The decrease in split tensile strength led to the increased porosity of matrices containing wood ash [60]. On the other hand, some studies report improvements when up to 25 wt% wood ash was used [41,61].

Regarding the flexural strength, the incorporation of wood ash generally decreases it [6,19,29,58,62], but there are cases where improvements occur at later ages [30]. Concrete with higher wood ash content tends to exhibit lower flexural strength due to poor bonding with the matrix. To maintain acceptable flexural strength, limiting the wood ash replacement ratio to 20% is recommended, especially for ashes with high silica content [63].

2.2.3. Durability properties

Generally, an increase in the wood ash ratio leads to higher water absorption [23,27,39]. Udoeyo et al. [19] studied various ash replacement levels (5-30 wt%) and observed a corresponding rise in water absorption with higher ash content. For instance, samples with 5, 15, and 30 wt% ash had water absorption ratios of 0.4%, 0.8%, and 1.05%, respectively, while below 10% for water absorption is an acceptable for most construction materials [19]. The water absorption capacity in mixes with wood ash was also affected by the water-to-cement ratio, with higher ratios resulting in increased water absorption [41]. However, Elinwa and Ejeh [54] reported the opposite effect, where the addition of 15 wt% sawdust ash reduced the water absorption in their study. The water absorption ratio decreased from 1.29% in the control sample to 0.8% in samples containing sawdust ash.

Low drying shrinkage is desirable as it reduces the formation of microcracks in concrete [58,64]. Cheah and Ramli [64] studied mortars with high-calcium wood ash and observed a significant reduction in drying shrinkage at 5 wt% wood ash content. However, at higher replacement ratios (15-25 wt%), the shrinkage increased compared to the reference sample. Carević et al. [32] investigated pastes and mortars with varying amounts of wood ash from different combustion technologies. They found that wood ash reduced the drying shrinkage regardless of the replacement ratio and combustion technology, but concerns were raised about free CaO formation at temperatures above 900 °C for the combustion technology, potentially affecting long-term properties. On the other hand, Candamano et al. [62] reported that wood ash increased drying shrinkage and weight loss, especially at a 30 wt% cement replacement ratio. The contribution of autogenous shrinkage decreased with lower cement content and higher wood ash content, with increased shrinkage attributed to hygrometric shrinkage, supported by higher weight loss.

In regions with cold climates, concrete undergoes freezing and thawing cycles, causing internal stress, microcracks, and reduced strength development by 20-40% due to slower hydration rates [65,66]. A high LOI negatively affects the efficiency of air-entraining admixtures, which help resist freezing and thawing [25]. Naik et al. [58] reported incorporating wood ash as a cement replacement at 5 wt%, 8 wt%, and 12 wt% has shown no significant impact on the frost resistance of concrete [17]. Wang et al. [67] examined various concrete mixes containing different ash combinations. They observed that the weight loss in samples with Class C fly ash was either equal to or lower than the reference sample, suggesting wood ash had a limited effect on

frost durability. Furthermore, the study ranked the air-entraining agent requirement as follows: Class F > Wood F > Wood C > Class C > pure Portland cement.

In concrete, high permeability enables rapid movement of ions and moisture, making it vulnerable to chemical erosion and attacks. The rapid chloride permeability is influenced by factors such as the water/binder ratio, curing conditions, and age of the concrete. Wang et al. [67] compared wood fly ash and coal fly ash as partial cement replacements and found that concrete containing wood ash demonstrated significant chloride permeability, mainly due to the larger particle size of the wood ash. Similarly, Garcia and Sousa-Coutinho [30] reported slightly higher chloride permeability in samples with 5 wt% and 10 wt% wood ash replacement, categorizing them as having a low level of resistance to chloride permeability.

Alkali-silica reaction (ASR) is a phenomenon in concrete where reactive silica in aggregates reacts with alkalis from the pore solution, leading to the formation of an alkali-silica gel. This gel expands upon exposure to water, which can cause cracks in the concrete [68,69]. High alkali content and LOI increase the risk of ASR expansion [67]. Various studies suggest that the inclusion of wood ash can mitigate ASR and its associated expansion. When wood ash is used as a cement replacement in mortar samples, ASR expansion is reduced. Esteves et al. [70] observed that higher amounts of wood ash led to a decrease in ASR expansion, and the addition of metakaolin further enhanced this effect. Similarly, Ramos et al. [6] reported significant reductions in ASR expansion with 10 wt% and 20 wt% wood ash replacements. Wang and Baxter [67] emphasized that biomass fly ash, despite having a higher alkali content than Class C coal fly ash, achieved a higher reduction in expansion. In fact, the expansion was limited to 0.1% after 6 months in mixes containing biomass fly ash, while Class C fly ash exceeded the expansion limit given in ASTM C33 [71].

2.3. Use of wood ash in alkali-activated systems

Alkali-activated binders, solidify through a chemical reaction between an aluminosilicate precursor and alkali activators. The primary reaction product is the formation of Calcium Alumina Silicate Hydrate gel (C-A-S-H), responsible for strength development in high calcium systems [72,73]. Alkali-activated materials are promising alternatives for traditional Portland cement-based systems due to their remarkable reduction in CO_2 emissions, reaching up to 80% [74–76]. These materials also demonstrate a 43% decrease in energy consumption and approximately 25% less water usage [77,78]. Furthermore, they exhibit improved strength and superior

durability characteristics [79,80]. Another advantage is their ability to utilize industrial waste materials and by-products such as slag or fly ash [81]. Ground granulated blast furnace slag (GGBFS) which is an industrial by-product from steel production is widely used as an alkali-activated precursor. While alkali-activated slag systems demonstrate high mechanical strength, they face challenges such as rapid setting times and high shrinkage. To address these issues, researchers have explored combining them with other precursors, resulting in promising enhancements. Among the binary systems studied, the combination of slag and fly ash is the most thoroughly investigated [79].

Apart from using wood ash as a partial replacement for cement, there is an increasing research interest in its application in alkali-activated materials. Some researchers have proposed using wood ash as an alkaline source for alkali-activated materials instead of chemical alkali solutions, considering the potential negative environmental impacts of substances like sodium silicate and sodium hydroxide. For instance, Cheah et al. [82] successfully replaced fly ash with varying amounts of wood ash (50 wt%, 60 wt%, 70 wt%, and 100 wt%) without the use of any alkali activator. They achieved a maximum compressive strength of 18 MPa with 60 wt% wood ash after 90 days. The high content of K2O and CaO in wood ash makes it suitable for geopolymerization. The reaction with water resulted in the formation of K-A-S-H, C-A-S-H, and C-S-H. Similarly, Samsudin and Cheah [83] investigated the use of high-calcium wood ash as a substitute for ground granulated blast furnace slag (GGBFS) in geopolymer concrete without any chemical alkali activator. A replacement ratio of 30% yielded the highest compressive strength at 12.3 MPa, with rapid early-stage strength development attributed to the high alkalinity of wood ash.

In addition to utilizing wood ash as an alkaline source, it has the potential to be used as a partial replacement for fly ash, metakaolin, and GGBFS in various applications. Owaid et al. [81] suggested that up to 25 wt% wood ash can be used as a partial replacement for fly ash in geopolymer concrete to improve cost-effectiveness and environmental sustainability. Different wood ash ratios (25 wt%, 50 wt%, 75 wt%, and 100 wt%) were compared using sodium silicate and sodium hydroxide as activators. The geopolymer concrete with 25 wt% wood ash replacement showed the highest compressive strength on the 56th day, which was 57.82 MPa, but higher wood ash ratios resulted in decreased mechanical properties, likely due to the high CaO content in wood ash. Similarly, Abdulkareem et al. [84] observed that the incorporation of up to 20 wt% wood ash as a partial replacement for fly ash in geopolymer mortars resulted in shorter initial and final setting times and improved early-age compressive strength. This improvement was attributed to

the formation of C-S-H (calcium-silicate-hydrate) and geopolymer gels during the geopolymerization process. Cheah et al. [85] studied the substitution of fly ash with high-calcium wood ash at different ratios in geopolymer mortars. They utilized a sodium silicate solution as an alkali activator with an alkali modulus of 2.1. The study revealed that the highest compressive and flexural strength was measured with 40 wt% and 50 wt% wood ash replacements at 7 and 28 days, respectively. Moreover, the samples containing 30 wt% wood ash exhibited the highest mechanical strength after 365 days.

Candamano et al. [86] conducted a study to assess the effect of utilizing wood ash as a partial replacement for metakaolin in geopolymer mortars. The addition of 10-30 wt% wood ash led to an improvement in workability, while exceeding 10 wt% replacement resulted in reduced compressive and flexural strengths. Nevertheless, even with a 30 wt% replacement ratio, the strength remained above 35 MPa, highlighting the potential of wood ash in geopolymer applications. De Rossi et al. [87] examined the influence of different curing methods on the properties of geopolymer mortars containing 75 wt% wood fly ash and 25 wt% metakaolin. The study employed two different ratios of sodium silicate to sodium hydroxide and subjected the samples to five curing methods. The findings revealed that a higher sodium silicate to sodium hydroxide ratio enhanced compressive strength and reduced water absorption, except for hydrothermal curing. The highest compressive strength of 24.5 MPa was observed in geopolymers cured at 40 °C; however, this method was not recommended due to increased carbon dioxide emissions and energy consumption. Room temperature curing was identified as a cost-effective and environmentally friendly alternative, yielding geopolymers with comparable mechanical properties.

Silva et al. [88] explored the utilization of untreated wood ash as a precursor, combined with NaOH solution as an alkali activator at varying concentrations. The samples containing 100 wt% wood ash displayed a porous and heterogeneous structure with microcracks, attributed to drying during curing and the large particles of wood ash. To enhance the mechanical properties, the authors suggested pre-treatments such as sieving and crushing for wood ash. Bajare et al. [89] investigated the use of wood ash as a precursor, which was ground with a planetary ball mill for 10 minutes to enhance its reactivity. They utilized a 6 M NaOH solution as the alkali activator. After curing the geopolymer mortars at 75 °C for 24 hours, they achieved a compressive strength of 9.3 MPa. Ates et al. [90] studied the influence of calcination and ball milling on the compressive and flexural strength of fly ash and wood ash blended geopolymer mortars. They observed that these processes

significantly improved the strength properties of the mortars, especially up to a 50 wt% wood ash ratio.

3. Methodology

In this chapter, materials and methods are described. Materials and related experiments are given in Table 1.

Table 1. Studies and related experiments with materials

Study	Description	Materials	Tests
Study A	Use of wood which is ground with different ball milling parameters as precursor in alkali-activated mortars	• WFA1	• Compressive strength
Study B	The use of wood ash as fly ash replacement in alkali-activated mortar	• WFA2 • Fly ash	• Compressive strength
Study C	Effects of ball milling on the pozzolanic property of wood ash	• WFA3 • Portland cement • Fly ash	• Frattini test • Compressive strength • Strength Activity Index (SAI)
Study D	The use of wood ash as slag replacement in alkali-activated mortars	• WFA3 • GGBFS	• Compressive strength • Flexural strength • SEM and EDS • XRD analysis • Isothermal calorimetry

3.1. Materials

3.1.1. Wood ash

Three different types of wood fly ashes were used in this project, WFA1, WFA2, WFA3, and all were obtained from Stenvalls Trä AB (Piteå, Sweden). They are a by-product of timber waste combustion and collected at different times. WFA1 and WFA2, were only used in preliminary studies, Study A and B, due to only small amounts being available. WFA3 represents unsieved wood fly ash 3 while -0, -10 and -20 denote the duration of milling in minutes.

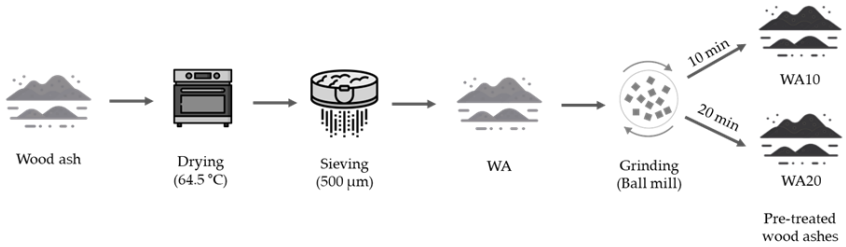

Figure 1. Processing of wood ash after receiving in Study D (Teker Ercan et al. [91]).

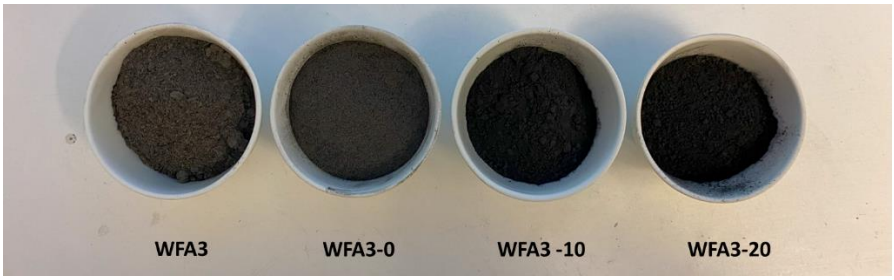

Figure 2. Untreated and ball milled WFA3, -10 and -20 denotes the duration of ball milling in minutes.

3.1.2. Ground granulated blast furnace

Ground granulated blast furnace slag (GGBFS) used in this project was sourced from SweCem (Helsingborg, Sweden) and its chemical composition is given in Table 1. The basicity coefficient (Kb) of GGBFS was calculated based on the equation Kb = (CaO + MgO)/(SiO_2 + Al_2O_3) and found to be 1.13, indicating that the GGBFS has a basic nature, as the value is greater than 1 [76,92–94]. The pH value of GGBFS was measured to be 10.38. The hydration modulus (HM) of the slag was calculated as 1.82 using the equation HM = (CaO + MgO + Al_2O_3) / SiO_2 [93]. The obtained HM value suggests that the hydration of slag is efficient, as it is greater than the recommended threshold of 1.4 for ensuring effective hydration product formation [93,95].

Table 2. Chemical composition of WFA3, WFA3-10, WFA3-20, GGBFS, CEM I 42.5 N and FA

Oxides (%)	WFA3-0	WFA3-10	WFA3-20	GGBFS	CEM I 42.5 N
SiO_2	22.40	22.30	21.70	34.80	21.20
Al_2O_3	6.75	6.87	6.77	11.30	3.40

Fe_2O_3	2.62	3.11	3.39	0.42	4.12
CaO	15.10	16.00	15.60	40.80	63.30
K_2O	8.25	8.96	9.27	0.99	0.56
MgO	2.69	2.84	2.84	11.40	2.20
MnO	0.80	0.85	0.82	0.32	-
P_2O_5	2.81	2.96	2.97	<0.02	-
TiO_2	0.30	0.30	0.28	1.46	-
Na_2O	1.46	1.48	1.47	0.58	0.18
LOI (1000 °C)	29.70	32.30	31.30	-1.81	2.50

3.1.3. Portland Cement

Portland cement (CEM I 42.5 N) was obtained from Cementa (Skövde, Sweden).

3.1.4. Fly ash

Australian fly ash (Type F) was obtained from Thomas Cement from Bremen, Germany.

3.1.5. Alkali activators

In Study A and B, the liquid sodium silicate (SS) (Na_2SiO_3) used was obtained from Sigma-Aldrich, and its alkali modulus (Ms) was calculated as Ms = SiO_2/Na_2O of 2.5, with 26.5 wt% SiO_2, 10.6 wt% Na_2O, and a solid content of 43.82 wt%. The Ms value was adjusted to given value in Table 3, Table 4 and Table 5 by adding sodium hydroxide (NaOH) pellets (98% purity) which was provided by Sigma-Aldrich.

Three different alkali activators were employed in alkali-activated mortars (Study D): sodium silicate (SS), sodium carbonate (SC), and sodium hydroxide (SH). Same liquid SS was used in this study and the alkali activator dosage for all SS-activated mixes was 10 wt% with Ms value 1.

Sodium carbonate (SC) powder (Na_2CO_3) used in the study was supplied by CEICH SA in Warsaw, Poland. 10 wt% SC was utilized in all SC-activated mixes.

For the SH-activated mixes, a 10 M concentration of sodium hydroxide (NaOH) solution was prepared using distilled water.

3.1.6. Aggregates

Fine sand B35 (350 μm) was used in the mortar samples and was supplied by Baskarpsand AB (Habo, Sweden) (Study A, C, and D).

Graded standard sand (0-4 mm) was used in the mortar mixes for determining the SAI and was obtained from the Jehander Heidelberg Cement Group (Study C).

3.2. Methods

3.2.1. Ball milling

The WFA1 was subjected to grinding using a planetary ball mill operating at a rotation speed of 500 rpm. Different ball-to-powder (b/p) ratios of 5, 10, and 15 were used during the grinding process. The duration of the grinding was set to 20 minutes for each b/p ratio. Loss on ignition (LOI) values for WFA1-5 and SWFA1-5 were 51.4% and 30%, respectively.

For the WFA2, the grinding process was conducted using the b/p ratio of 5 and the rotation speed of 500 rpm, with duration of 20 minutes.

Regarding the WFA3, the grinding process was performed with the same b/p ratio of 5 and rotation speed of 500 rpm, but with varying durations of 10 minutes and 20 minutes.

The equipment used for all grinding procedures was a Retsch PM100 planetary ball mill, manufactured by Retsch GmbH in Haan, Germany (Figure 3a). The jar had a capacity of 500 mL, and 10 stainless steel balls with a diameter of 20 mm (Figure 3b) were used during each grinding operation.

Figure 3. (a) Planetary ball mill, Retsch PM 100, (b) grinding media with 20 mm diameter

3.2.2. Mixing

In Study A, the design of the alkali-activated wood ash mortar is presented in Table 3. Initially, the dry materials were mixed for 3 minutes, and subsequently, the SS solution was added and mixed for an additional 2 minutes using the Ecovac Bredent small volume vacuum mixer (Figure 4). Small beam molds with dimensions of 1.2 x 1.2 x 6 cm^3 (Figure 5a) were used for casting. Samples were kept in ambient conditions after demoulding.

For study B, mortar design and curing regime are given in Table 4. The same mixing procedure was used as in the Study A. However, a Hobart mixer and cube molds with dimensions of 50x50x50 mm^3 (Figure 5b) were used for mixing and casting.

For the Study C, the control mixture with 100 wt% Portland cement and test mixtures with 20 wt% wood ash or fly ash were prepared according to the ASTM C–311 [37]. Graded standard sand (0-4 mm) was used in the mortar mixes with s/b ratio 2.75 and w/b ratios were 0.48 for the control sample and 0.5 for the test samples. Mixing was done using a Hobart mixer, where dry materials were blended for 3 minutes, followed by the addition of water, and mixing for an additional 2 minutes. The casting was carried out in cube molds with dimensions of 50x50x50 mm^3 (Figure 5b). After 24 hours, all samples were demoulded and submerged in a water bath until the day of testing.

Mortar samples were utilized for conducting compressive and flexural strength tests, as well as for SEM and EDS spot analysis. A total of 21 different alkali-activated mortar mixes were prepared for the Study D, with varying proportions of the Ground Granulated Blast Furnace Slag (GGBFS) replaced by the untreated wood ash (WA) and the ground wood ash (WA10, WA20). The mix designs for the alkali-activated mortars are given in Table 5. In the mortar ID, the first number after the alkali-activator code denotes the wood ash ratio in the mix, while the second number represents the grinding duration. Control mortar samples were also prepared, using 100 wt% GGBFS for all three types of alkali activators. For all mortar mixes, the w/b and s/b ratios were fixed at 0.5 and 2, respectively. Solutions of sodium silicate (SS) and sodium hydroxide (SH) were prepared approximately 3 hours prior to casting.

The mixing process involved initially mixing dry materials in a Hobart mixer for three minutes. Subsequently, the alkali activators dissolved in water were added, and the mixture was mixed for an additional two minutes. The samples were then cast into moulds with dimensions of 40 x 40 x 160 mm^3 (Figure 5c) and sealed with plastic foil before being stored under ambient conditions. Upon demoulding, all

samples were kept sealed in plastic bags. Demoulded samples were given in Figure 6.

For XRD analysis and isothermal calorimetry measurements, paste samples were prepared. The pastes were mixed for 2 minutes using a small volume vacuum mixer of type Ecovac Bredent (Senden, Germany), Figure 4, at a mixing speed of 600 rpm.

Table 3. Alkali-activated wood ash mortars mix design for the Study A.

Mortar Mix ID	b/p ratio for wood ash	Wood ash ratio (%)	Alkali activator type	Alkali activator dosage	Alkali modulus (Ms)	Type of Curing
WFA1-5	5	100	SS	10%	1	Ambient
WFA1-10	10	100	SS	10%	1	Ambient
WFA1-15	15	100	SS	10%	1	Ambient
SWFA1-5	5	100	SS	10%	1	Ambient
SWFA1-10	10	100	SS	10%	1	Ambient
SWFA1-15	15	100	SS	10%	1	Ambient

WFA1: Wood Fly Ash 1; SWFA1: Sieved Wood Fly Ash 1

Figure 4. Ecovac Bredent small volume vacuum mixer

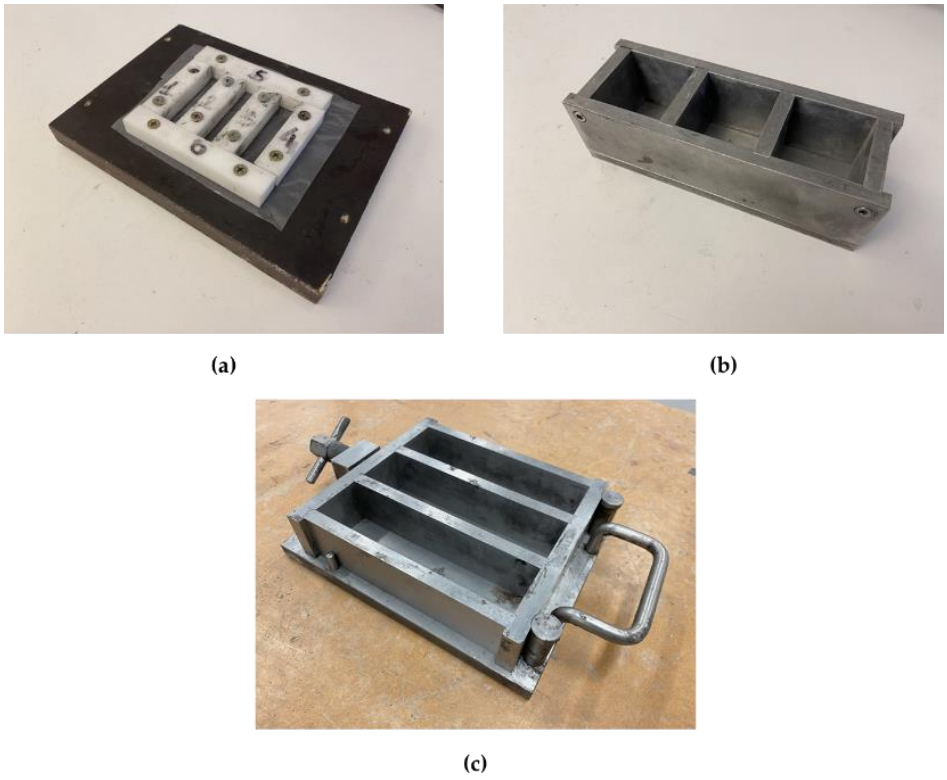

Figure 5. The moulds having dimension of (a) 12 x 12 x 60 mm^3, (b) 50 x 50 x 50 mm^3 (c) 40 x 40 x 160 mm^3.

Table 4. Alkali-activated mortar mix designs for the Study B.

Mortar Mix ID	Fly ash:wood ash ratio	Alkali activator type	Alkali activator dosage	Alkali modulus (Ms)	Type of Curing
FA0	100:0	SS	10%	1	Water
FA-WFA2	90:10	SS	10%	1	Water
G-FA-SWFA2(0.25)	90:10	SS	10%	0.25	Water
G-FA-SWFA2(0.5)	90:10	SS	10%	0.5	Water
G-FA-SWFA2(1.25)	90:10	SS	10%	1.25	Water
FA0	100:0	SS	10%	1.5	80°C
FA0	100:0	SS	10%	2	80°C

FA0	100:0	SS	10%	2.5	80°C
G-FA-SWFA2(1.5)	90:10	SS	10%	1.5	80°C
G-FA-SWFA2(2)	90:10	SS	10%	2	80°C
G-FA-SWFA2(2.5)	90:10	SS	10%	2.5	80°C

G: fly ash and wood ash ground together; WFA2: Wood Fly Ash 2

Table 5. Alkali-activated mortar mix designs for the Study D (Teker Ercan et al. [91]).

Mortar Mix ID	Wood ash grinding time (min)	Slag:wood ash ratio	Alkali activator type	Alkali activator dosage	Alkali modulus (Ms)	pH of alkali solution
SS-CTRL	-	100:0	SS	10%	1	12.84
SS-10	0	90:10	SS	10%	1	12.84
SS-20	0	80:20	SS	10%	1	12.84
SS-10-10	10	90:10	SS	10%	1	12.84
SS-20-10	10	80:20	SS	10%	1	12.84
SS-10-20	20	90:10	SS	10%	1	12.84
SS-20-20	20	80:20	SS	10%	1	12.84
SC-CTRL	-	100:0	SC	10%	-	11.24
SC-10	0	90:10	SC	10%	-	11.24
SC-20	0	80:20	SC	10%	-	11.24
SC-10-10	10	90:10	SC	10%	-	11.24
SC-20-10	10	80:20	SC	10%	-	11.24
SC-10-20	20	90:10	SC	10%	-	11.24
SC-20-20	20	80:20	SC	10%	-	11.24
SH-CTRL	-	100:0	SH	10 M	-	12.95
SH-10	0	90:10	SH	10 M	-	12.95
SH-20	0	80:20	SH	10 M	-	12.95
SH-10-10	10	90:10	SH	10 M	-	12.95
SH-20-10	10	80:20	SH	10 M	-	12.95
SH-10-20	20	90:10	SH	10 M	-	12.95
SH-20-20	20	80:20	SH	10 M	-	12.95

SS: Sodium silicate, SC: Sodium carbonate, SH: Sodium hydroxide.

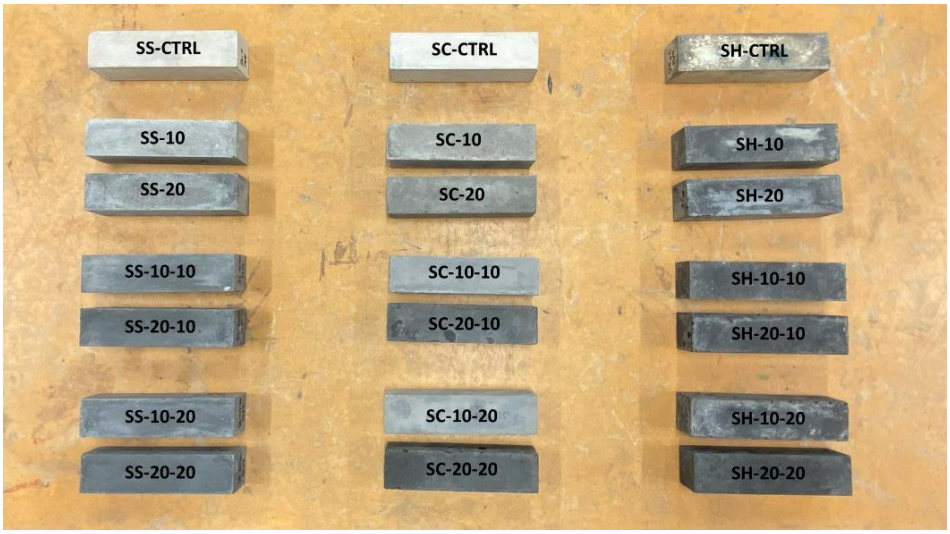

Figure 6. Alkali-activated mortar beams for the Study D.

3.2.3. Compressive strength

The compressive strength measurement was done 7 days after casting with the force applied to an area of 10 x 10 mm^2 using a Wykeham Farrance mechanical testing machine, Figure 7b (Study A).

The compressive strength test was performed in an area of 40 x 40 mm^2 from both ends of each mortar beam for the samples at 7 and 28 days (Study D) [96]. A Toni Technik compression machine was used for these measurements (Figure 7a).

3.2.4. Flexural strength

The flexural strength of the mortar samples was determined at 7 and 28 days according to the BS EN 196-1:1995 [97]. A Wykeham Farrance mechanical testing machine which is shown in Figure 7b was employed for these measurements, using a loading speed of 0.5 mm/min and was controlled by the Catman Easy software.

Figure 7. (a) Toni Technik compression machine, (b) Wykeham Farrance mechanical testing machine

3.2.5. Strength Activity Index (SAI)

The SAI was assessed by conducting comparative compressive strength tests on mortar cubes with dimensions of 50x50x50 mm^3 at the age of 7 and 28 days. According to the ASTM C618 [26], a material can be classified as having pozzolanic reactivity if the SAI is higher than 75% for both 7 and 28 days.

$$SAI\ (\%) = \frac{A}{B}\ x\ 100$$

Where A is the compressive strength value of the 20 wt% wood ash or fly ash containing mortar cube and B is the compressive strength of the 100 wt% control mortar cubes.

3.2.6. Frattini test

The Frattini test for an indication of the pozzolanic reactivity of wood ash was performed according to EN 196-5 [98]. The samples were prepared as a mixture of 80 wt% PC and 20 wt% of wood ash or fly ash. The control sample was prepared with 100 wt% PC. All samples were mixed with 100 ml of distilled water, which was boiled initially and stored in the oven at 40°C in the closed containers. Then, the test samples were kept in the oven at 40°C for 15 days. On the test day, the suspension of the samples was vacuum filtered through filter paper. Subsequently, 50 ml of the filtrated solution was titrated with 0.1 M hydrochloric acid (HCl) using methyl orange as the indicator. Subsequently, [Ca^{2+}] ions were titrated with a 0.3 M EDTA solution using Patton and Reeder's indicator. The concentrations of hydroxyls and [Ca^{2+}] ions are then plotted on a graph, representing the relationship between CaO concentration and [OH^-] ion concentration [99–101].

3.2.7. Scanning Electron Microscopy (SEM) and EDS analysis

For the SEM analysis of Study D, mortar pieces were extracted from the core of the samples at the age of 28 days. The pieces were stored in isopropanol for 48 hours to stop ongoing chemical reactions. Subsequently, the samples were placed in a desiccator for an additional 48 hours to ensure complete drying.

In the following step, the samples were impregnated with a low-viscosity epoxy resin (Struers EpoFix) under vacuum, utilizing Struers CitoVac equipment (Figure 8a). Once the epoxy resin had solidified, the samples underwent polishing using grinding plates coated with a diamond spray containing particle sizes of 9, 3, and 1 μm, utilizing Struers LaboForce-100 (Figure 8b). Lamp oil was used as a lubricant during the polishing process [102].

The microstructure and morphology of both wood ashes and hardened alkali-activated mortar samples were analysed using a Scanning Electron Microscope model JSM-IT100 (JEOL Ltd, Tokyo, Japan) equipped with an energy dispersive spectrometer, BRUKER (JEOL Nordic AB, Sollentuna, Sweden), and analyzed with ESPRIT 2 software (Figure 9).

The SEM analysis was conducted using a backscattered electron detector (BSE) in low vacuum mode, with an accelerating voltage of 15.0 kV and a probe current of 50 mA at 500x magnification. For EDS spot analysis, 100 points were manually selected based on the grey level histogram corresponding to C-S-H, and the analysis was performed at a magnification of 1000x [102].

To estimate the approximate porosity, SEM images were analyzed using the ImageJ software [103]. The images at 500x magnification were captured at multiple locations. Gaussian filtering was applied to all analyzed images to reduce noise levels and enhance the contrast between hydration phases and pores. Subsequently, automatic thresholding was applied to convert the images into binary format.

The mean particle size was determined through the analysis of SEM images using ImageJ software. A median filter with a 2-pixel kernel was used to eliminate noise, and automatic thresholding was then applied to convert the images into a binary format for further analysis.

Figure 8. (a) Struers CitoVac, (b) Struers LaboForce-100.

Figure 9. Scanning Electron Microscope (SEM)

3.2.8. X-ray Diffraction (XRD)

X-ray diffraction (XRD) analysis was carried out on both, powdered samples and 7-day-old pastes of selected mixes (Study D). A PANalytical Empyrean X-ray diffractometer equipped with a PIXcel 3D detector was used. The operating conditions for the XRD analysis were set at 45 kV and 40 mA, with Cu-K radiation having a wavelength of 1.54 Å. The step size used for data collection was 0.02, and the scanning range of angles (2θ) ranged from 5° to 70° [28]. To determine the phase composition of the samples, the Crystallography Open Database (COD) was used.

3.2.9. Isothermal calorimetry

Isothermal calorimetry measurements were carried out using a TAM Air isothermal calorimeter which is given in Figure 10a. SS, SC and SH-activated paste samples containing 20 wt% of ground wood ash for 10 minutes 20 wt% of untreated wood ash, and 100 wt% slag-containing samples were selected for isothermal calorimetry measurement (Study D). Each paste sample weighed 8.3 g and was placed into a glass ampoule (Figure 10b). The samples were then maintained at a constant base temperature of 23 ± 0.02 °C for 7 days [104].

(a) (b)

Figure 10. (a) TAM Air isothermal calorimeter, (b) glass ampoules

4. Results and discussions

In this chapter, the results related to pozzolanic properties of wood ash and the mechanical properties and microstructure of the alkali-activated systems containing wood ash are presented and discussed.

4.1. Alkali-activated wood ash ground with different ball-to-powder ratios – *Study A*

The compressive strength of the alkali-activated wood ash mortars is given in Figure 11. The mortars containing ground wood ash with b/p ratio of 5 showed the highest values for both sieved and unsieved wood ashes. Although alkali-activated mortar samples containing unsieved wood ash showed higher compressive strength than those containing sieved ash, the optimum process and b/p ratio were determined as sieving and 5 due to the lower LOI of sieved wood ash compared to the other.

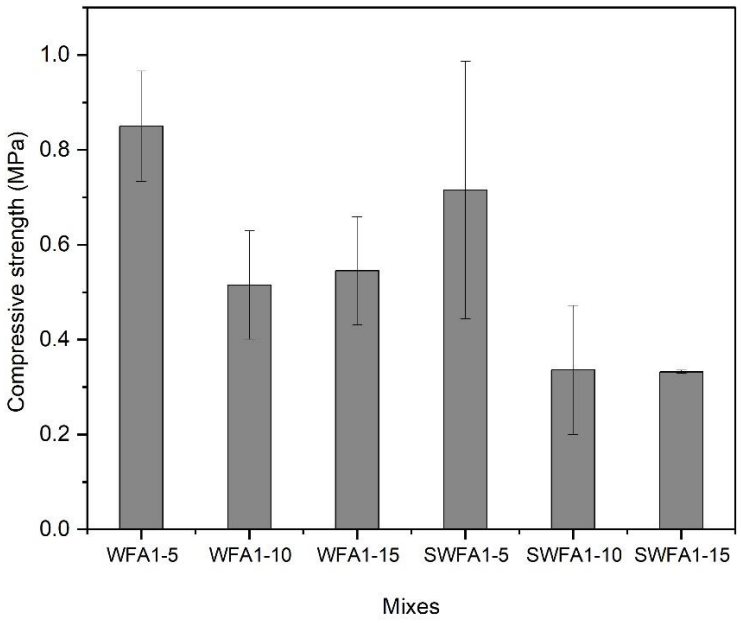

Figure 11. Compressive strength of alkali-activated wood ash mortars

4.2. The use of wood ash as fly ash replacement – *Study B*

The compressive strength test results for the samples subjected to water curing were inconclusive, as the samples "crumbled" during testing, and no measurable strength values were obtained. In an effort to enhance the curing process, a 24-hour heat cure at 80°C was applied to another set of samples. However, the exact duration of the exposure to the specified temperature remained uncertain due to the unexpected oven failure. Despite this, the heat-cured samples did not "crumble" like the water-cured samples during testing. Nevertheless, it is important to note that no compressive strength value was obtained from these heat-cured samples either. This suggests that the elevated temperature might have had a beneficial effect on the sample's structural stability.

4.3. Pozzolanic activity – *Study C*

The Frattini test results are given in Figure 12. According to EN 196-5 [98], test results located below the marked curve show pozzolanic reactivity. The test results located above the curve indicate non-pozzolanic materials. The control sample, which is 100 wt% Portland cement was located on the curve. FA, WFA3-10 and WFA3-20 exhibited pozzolanic reactivity while WFA3-0 did not. The results indicated that the used ball milling improved the pozzolanic properties of wood ash for both 10- and 20-minutes grinding durations. These results were also consistent with the SAI results which are given in Figure 13 except for FA. According to the ASTM C618 [26], the SAI should be higher than 75% for indication of pozzolanic reactivity. Ground wood ashes, which are WFA3-10 and WFA3-20, exceed the limit for SAI which is specified in ASTM C618 [26]. However, untreated wood ash (WFA3-0) and FA did not exceed 75%.

4.4. The use of wood ash as slag replacement – *Study D*

Table 2 presents the mean particle sizes of WFA3-0, WFA3-10, and WFA3-20. WFA3-0 had larger and more irregularly shaped particles compared to WFA3-10 and WFA3-20, as shown in Figure 14. Ball milling had a positive impact on reducing the wood ash particle sizes and achieving more uniform shapes. The mean particle size of WFA3-10 was smaller than that of WFA3-20, attributed to agglomeration, which significantly influenced the particle size distribution. Milling is known to decrease the particle size, but excessive milling beyond a critical time may have adverse the effect and cause agglomeration, leading to a wider particle size distribution, mainly occurring within the first hour of milling [105,106]. The initial 10 minutes of grinding were found to be crucial for particle size reduction, with diminishing effects afterwards [107]. Prolonged grinding processes might also resulted in more irregular particle shapes [106]. Smaller particles in the grinding media could cover the grinding balls and reduce milling efficiency over time [108]. Additionally, grinding media wear played a significant role in affecting grinding kinetics and overall milling efficiency [109].

Table 6. Ball milling parameters and mean particle size of WFA3-0, WFA3-10 and WFA3-20

Sample	Ball/powder ratio	Speed (rpm)	Milling Duration (min)	Mean particle size (μm)
WFA3-0	-	-	-	18.31
WFA3-10	5	500	10	3.79

WFA3-20	5	500	20	4.22

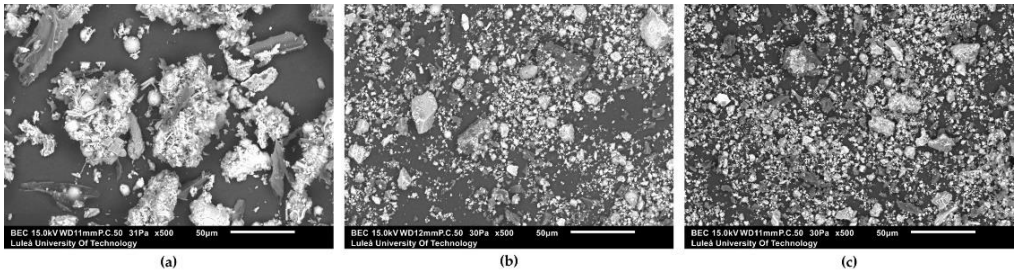

Figure 12. SEM images of (a) WFA3-0, (b) WFA3-10, (c) WFA3-20 at 500x magnification (Teker Ercan et al. [91]).

The XRD patterns for WFA3-0, WFA3-10, WFA3-20, and GGBFS are given in Figure 15. In the XRD patterns of ground wood ashes (WFA3-10 and WFA3-20), the dominant peak corresponded to quartz. This aligns with existing literature where quartz is frequently reported as the main crystalline phase found in wood ash [20,21,28,36,62,70,88,110]. Additionally, calcite, arcanite, and sylvite were also present in WFA3-10 and WFA3-20. On the other hand, the XRD pattern of untreated wood ash (WFA3-0) exhibited the main peak corresponding to calcite, while quartz peaks were observed with lower intensities, and arcanite was also detected. Moreover, akermanite was the primary phase of GGBFS.

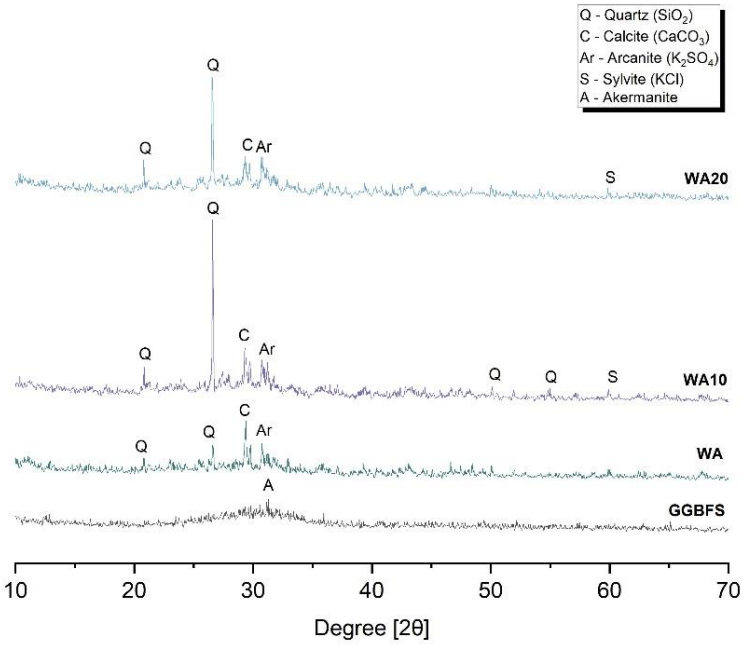

Figure 13. XRD analysis for WA (WFA3-0), WA10 (WFA3-10), WA20 (WFA3-20) and GGBFS (Teker Ercan et al. [91]).

4.4.1. Workability

Figure 16 shows the measured slump flow diameter values for all mixes. The results indicated that SS-activated samples exhibited a higher flowability than those activated with SC and SH. The control samples showed the highest flowability, with the order of flowability being SS > SC > SH. As the amount of wood ash and grinding time increased, the flowability decreased for all alkali-activator types.

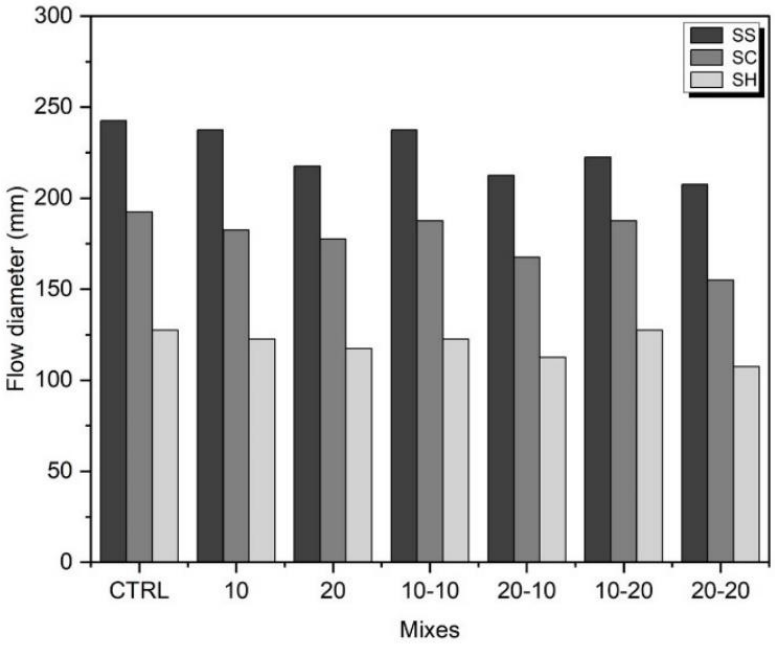

Figure 14. Flow diameter of alkali-activated mixes (Teker Ercan et al. [91]).

4.4.2. Mechanical properties

The compressive strength results at 7 and 28 days are presented in Figure 17. The results demonstrate that SS-activated samples exhibited the highest compressive strength values at both 7 and 28 days. Regardless of the alkali activator used and the grinding time of wood ash, it was observed that the compressive strength decreased with an increasing amount of wood ash. The addition of untreated wood ash led to a reduction in compressive strength compared to the control sample. This decrease was attributed to the high unburned carbon content and larger, unreactive wood ash particles [28,111]. The ground wood ash decreased the reduction of the compressive strength compared to the untreated wood ash due to its increased reactivity [40,112–114]. Moreover, SS-activated samples with a 10 wt% wood ash ratio and ground for 10 minutes (SS-10-10) achieved a compressive strength of 73.33 MPa at 28 days, with a slight increase of 3.5% compared to the control sample. This contribution was attributed to the high alkaline content of wood ash promoting the dissolution of aluminosilicate materials [83].

The strength development is governed by the C-A-S-H gel as the Ca/Al ratio achieves values greater than 2 [115]. Moreover, a lower Ca/Si ratio has been associated with positive effects on the mechanical properties of materials [116]. However, the presence of unreacted particles and porosity significantly influences the compressive strength of mortars. Silicon ions from an alkaline environment react with the calcium in the precursors to form C-S-H gel, supporting the formation of nucleation sites that contribute to the strength development [88]. In addition, fine particles of the ground wood ash further accelerated the hydration reactions, resulting in formation of more hydration products and reduced porosity [117].

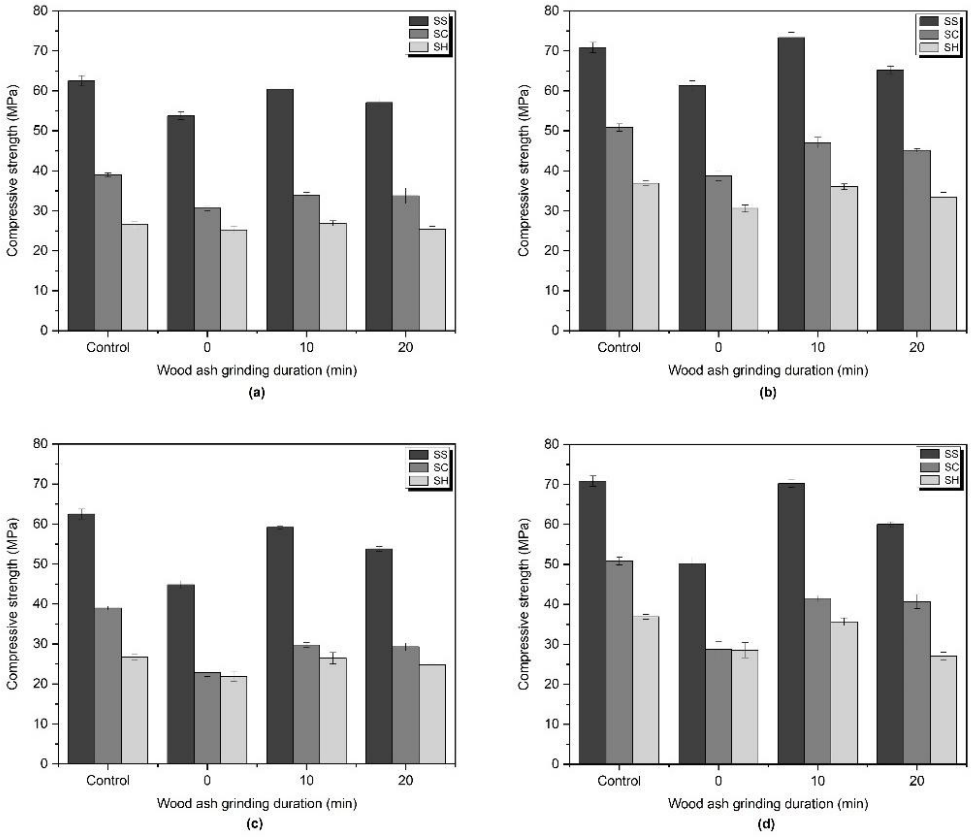

Figure 15. Compressive strength of alkali-activated mortars (Teker Ercan et al. [91]).

The flexural strength results for the alkali-activated mortars at 7 and 28 days are shown in Figure 18. Generally, the flexural strength exhibited a similar trend to

the measured compressive strength for each alkali activator type. Surprisingly, SH-activated samples demonstrated significantly higher flexural strength values. All SH-activated samples incorporating 10 wt% wood ash displayed higher flexural strengths compared to the control sample at 28 days, with SH-10-10 achieving the highest value of 19.19 MPa, representing an increase of 58.89%. The underlying cause of the surprisingly high flexural strength in SH-activated samples incorporating wood ash needs further investigation.

Lower flexural strength observed in SC-activated samples, in comparison to other activator types, can be attributed to the presence of microcracks and higher porosity. It is important to note that the flexural strength is more influenced by the presence of microcracks than the compressive strength [93].

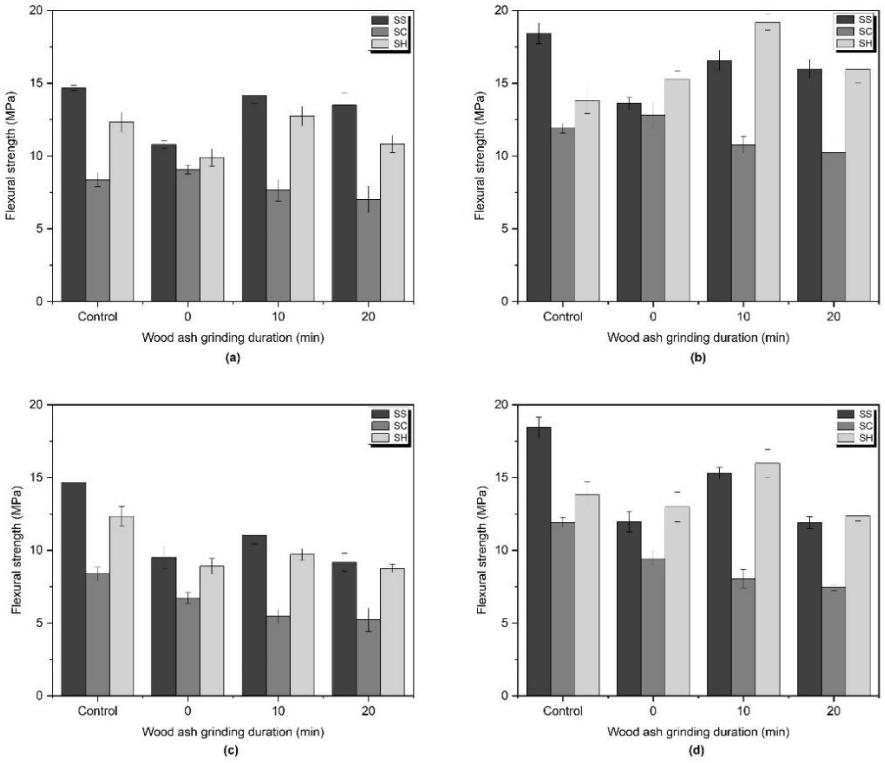

Figure 16. Flexural strength of alkali-activated mortars (Teker Ercan et al. [91]).

4.4.3. Microstructure

SEM analysis was performed to investigate the microstructure of the 28-day-old alkali-activated mortar samples. Micrographs of the specimens at 500x magnification were presented in Figure 19 and Figure 20. Both the control samples and those containing 10 wt% wood ash ground for 10 minutes exhibited a more uniform and denser microstructure, regardless of the alkali activator type used. However, an increase in the wood ash ratio led to the presence of more microcracks and unreacted GGBFS and wood ash. These microcracks might affect the mechanical strength and long-term durability of the material and are often associated with drying and shrinkage. The wood ash ground for 10 minutes showed better dispersion within the binder matrix compared to the samples containing wood ash ground for 20 minutes, where more unreacted wood ash particles were observed.

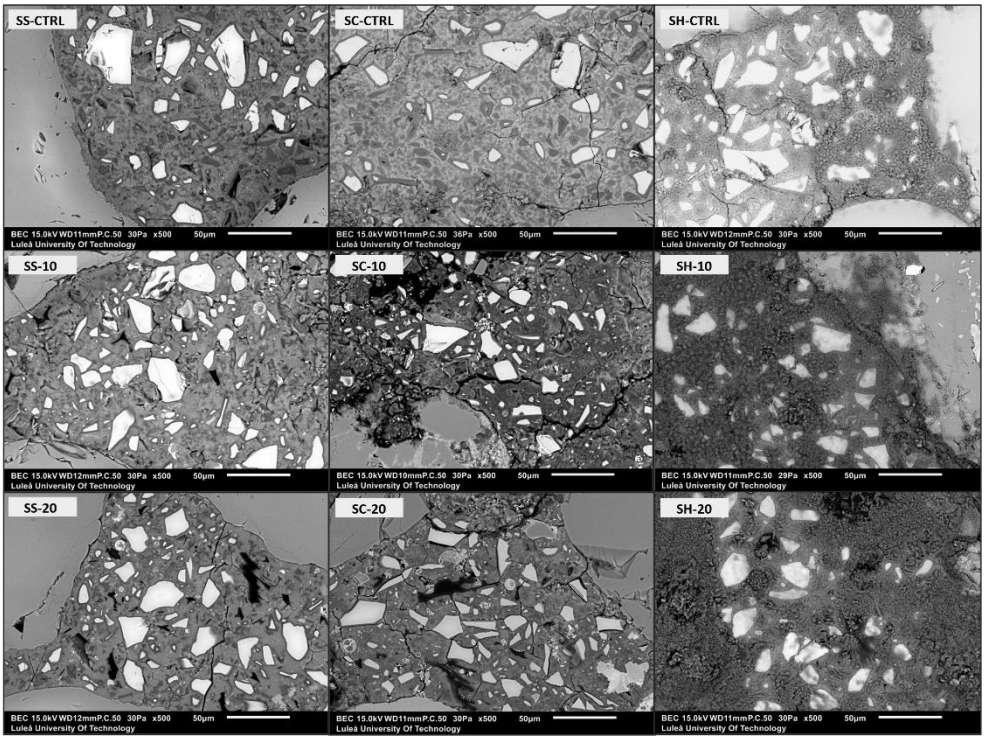

Figure 17. Micrographs of the 28 days old alkali-activated mortars at 500x magnification (Teker Ercan et al. [91]).

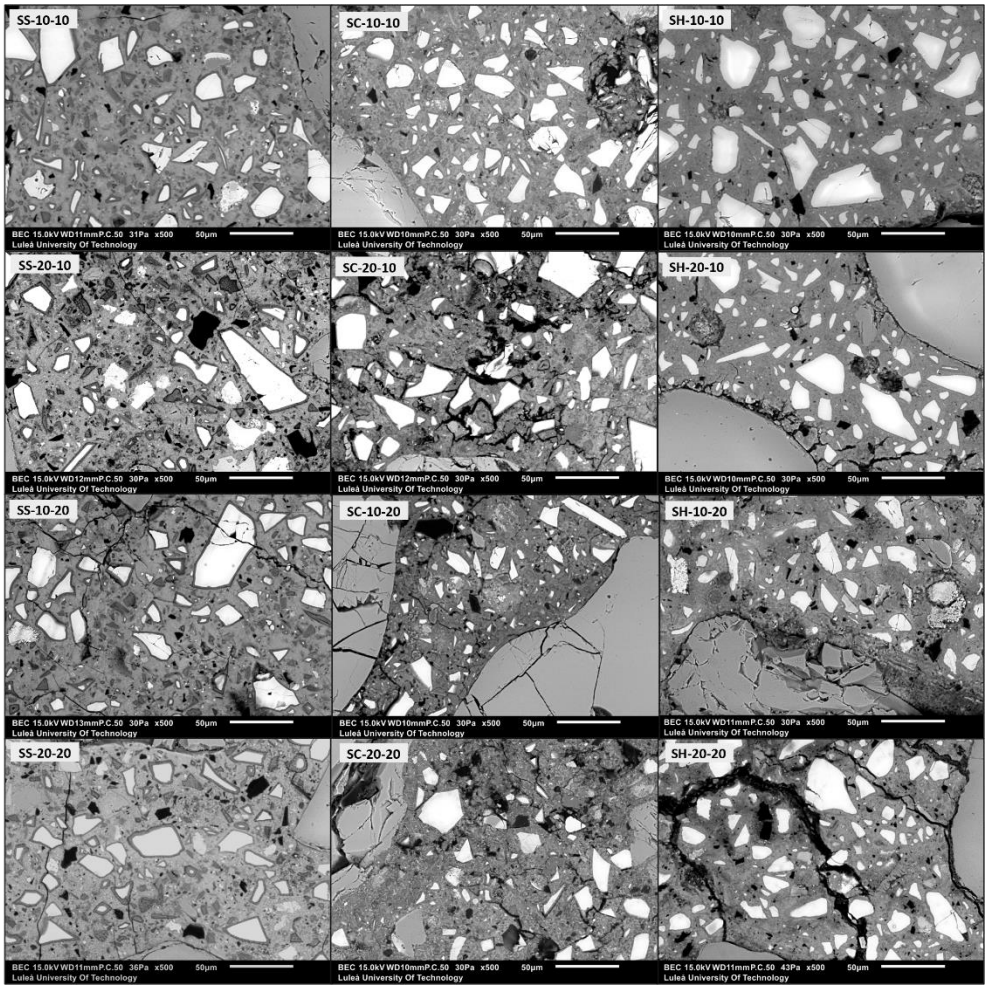

Figure 18. Micrographs of the 28 days old alkali-activated mortars at 500x magnification (Teker Ercan et al. [91]).

The total porosity of the alkali-activated mortars was estimated based on SEM micrographs, Figure 21. The addition of wood ash led generally to a higher porosity in the alkali-activated samples, irrespective of the type of alkali activator used [86,88]. According to Hu et al. [118], when fly ash was added, leading to increased porosity by reducing the content of the dense C-A-S-H gel and encouraging the formation of a high-porosity N-A-S-H gel. On the other hand, the SH-activated samples containing 10 wt% wood ash exhibited slightly lower porosity than the control sample, possibly due to limitations in the image analysis technique.

Additionally, the mortar samples containing WFA3-10 showed a slightly lower porosity compared to those with WFA3-20, likely due to the smaller particle size of WFA3-10 thus contributing to their improved reactivity.

When comparing the three alkali activator types, the SS-activated mortars showed lower porosity and denser microstructure than SC and SH-activated mortars. This lower porosity in SS-activated samples was attributed to the Si content in the medium [80]. However, the SH-activated mortars had slightly higher porosity compared to the SS-activated samples, yet still lower than the SC-activated samples. This difference was likely due to the higher pH value of the SS and SH solutions, which enhanced the dissolution of the GGBFS compared to other alkali activators, resulting in a denser matrix through pore filling [117].

Calculated average atomic ratios based on results obtained from EDS spot analysis for alkali-activated mortars are given in Figure 22. EDS spot analysis indicated that the primary hydration product was C-A-S-H gel, with Ca/Si atomic ratios ranged between 0.6 and 1.5, consistent with C-A-S-H gel characteristics [92]. Furthermore, the Ca/Si ratio of SS-activated mixes was lower compared to other activated samples, attributed to the increasing SiO_4^{4-} ions, promoting the formation of more hydration products which might enhance the alkali binding capability in C-A-S-H and accelerate the hydration process [117,119].

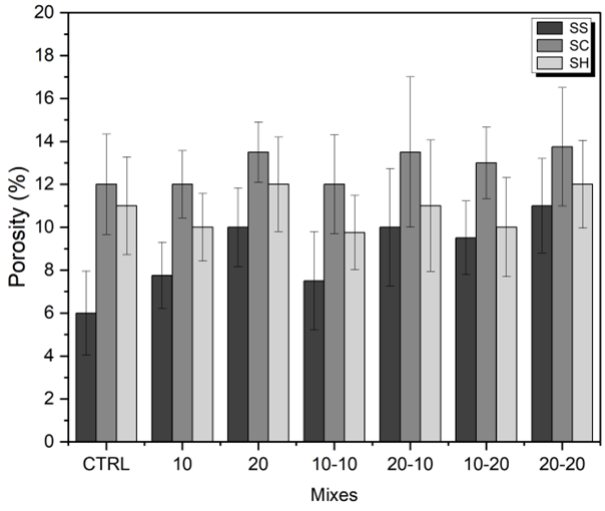

Figure 19. Estimated total porosity of the alkali-activated mortars (Teker Ercan et al. [91]).

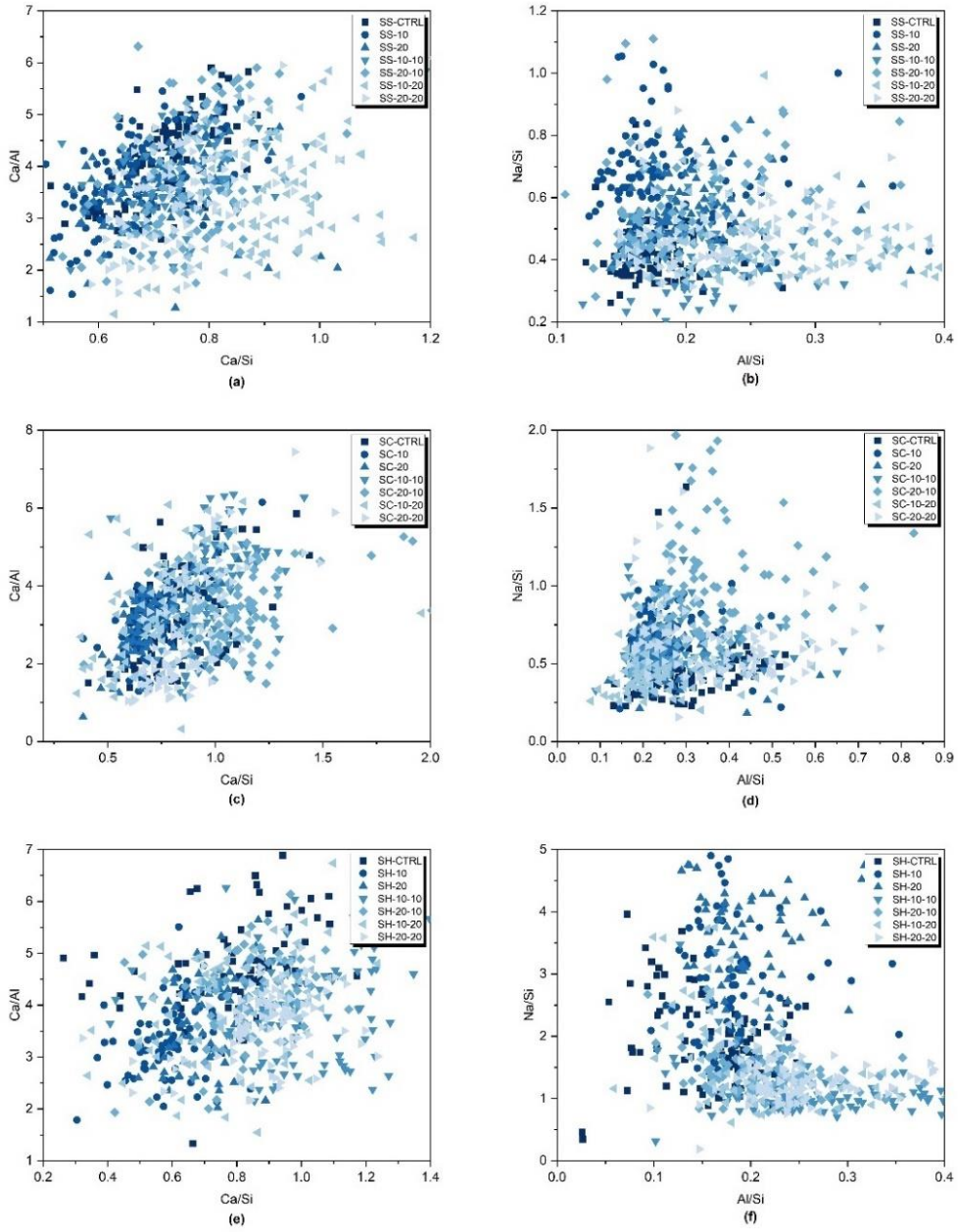

Figure 20. Calculated average atomic ratios based on results obtained from EDS spot analysis for alkali-activated mortars (adapted from Teker Ercan et al. [91]).

4.4.4. Phase development

The XRD patterns of alkali-activated pastes which are given in Figure 23, showed the presence of various crystalline phases during hydration. The main peak observed in all alkali activator types was identified as the C-A-S-H gel which was further supported by EDS spot analysis and consistent with previous research [117,120,121]. Common crystalline phases for all alkali-activator types included hydrotalcite and quartz. Moreover, akermanite in the SS-activated samples; gaylussite, portlandite, mullite, vaterite and akermanite in the SC-activated samples, and vaterite for SH-activated samples were observed.

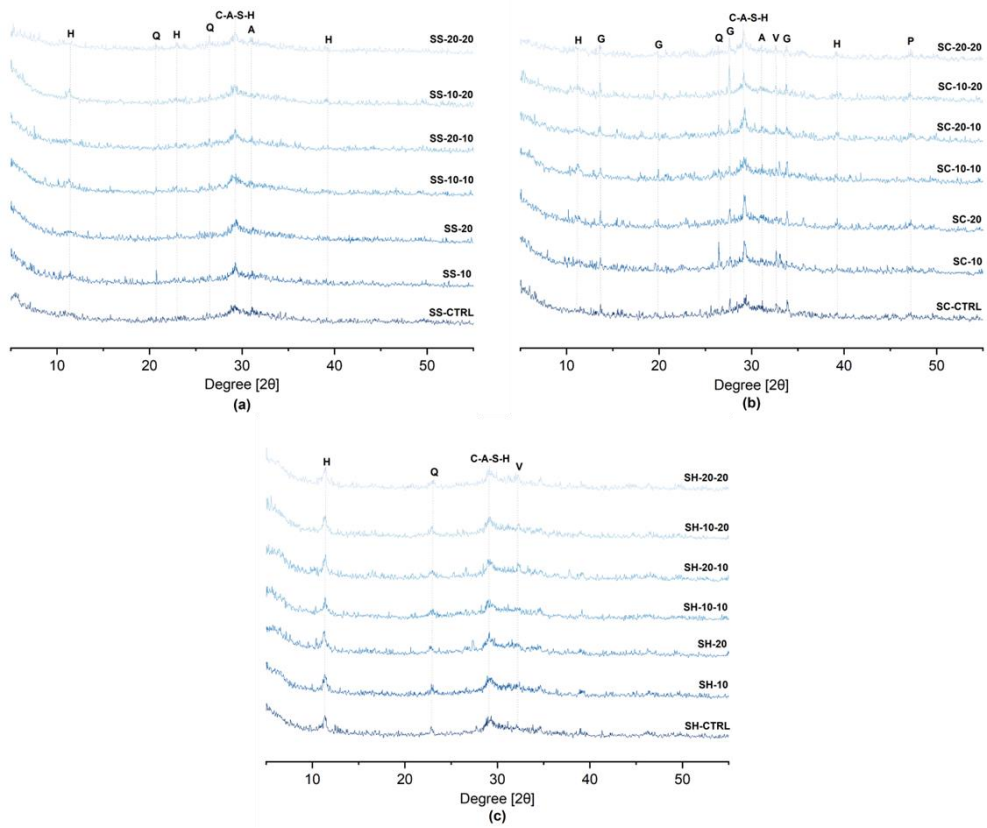

Figure 21. X-ray diffractograms of (a) SS-activated, (b) SC-activated, (c) SH-activated pastes at the age of 7 day (H – Hydrotalcite, G – Gaylussite, V – Vaterite, Q – Quartz, M – Mullite, A – Akermanite, P – Portlandite) (Teker Ercan et al. [91]).

4.4.5. Reaction heat development

To gain deeper insights into the reactions and phase development within the alkali-activated systems, isothermal calorimetry analyses were conducted on selected mixtures: SS-CTRL, SS-20, and SS-20-10; SC-CTRL, SC-20, and SC-20-10; SH-CTRL, SH-20, and SH-20-10 (Figure 24). Based on the results of the compressive strength tests, it was observed that samples incorporating wood ash ground for 10 minutes exhibited higher strength values across various replacement ratios and alkali activator types. Consequently, the mixes containing wood ash ground for 10 minutes (WFA3-10) were chosen for the calorimetry measurements. Although the highest compressive strength values were achieved with a 10 wt% wood ash content, the 20 wt% wood ash replacements were selected to better evaluate the effect of grinding. The heat development was monitored for a total of 168 hours.

The hydration process in geopolymers based on GGBFS involves five stages: dissolution, induction, acceleration, deceleration, and slow-down period [122,123]. Isothermal calorimetry results for selected SS-activated samples showed that the control sample (SS-CTRL) had a significantly higher first peak than SS-20 and SS-20-10, indicating a higher GGBFS depolymerization [124]. Grinding of wood ash did not significantly affect its dissolution rate in GGBFS. The SS-20-10 sample displayed an earlier and more intense second peak, suggesting a shortened induction stage due to wood ash incorporation. Its cumulative heat release at 168 hours was slightly higher than the control sample. Furthermore, a rare third peak was observed in SS-20-10, contributing to the increased cumulative heat, which might be attributed to the activator gelation or the initial formation of C-A-S-H [125].

In the SC-activated samples, the induction period was slightly delayed compared to the SS and SH-activated samples [117]. The second hydration peak of the slag was lower in intensity and significantly delayed [76]. The wood ash containing samples exhibited lower intensity peaks and slower hydration processes. SC-20-10 showed the highest cumulative heat release in the first 44 hours, while SC-CTRL had the highest cumulative heat of 160.5 J/g at 168 hours. The first peak of SC-20-10 was also notably higher compared to SC-CTRL and SC-20.

On the other hand, for SH-activated samples, the second peak did not occur, possibly due to the limited formation of reaction products within the paste during the 7-day period, as supported by the low intensity of the C-A-S-H peak in the XRD pattern.

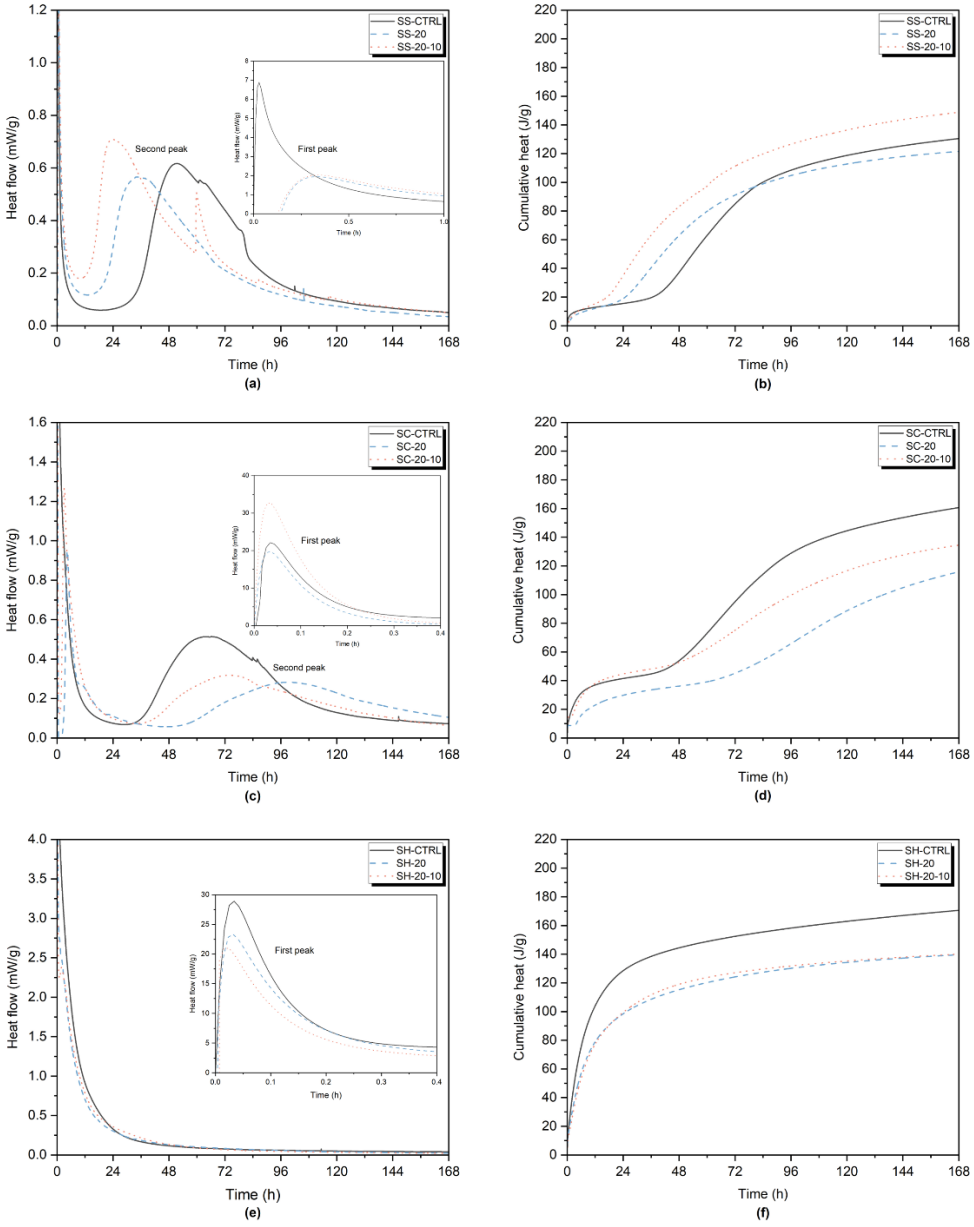

Figure 22. Heat flow of (a) SS-activated pastes, (c) SC-activated pastes, (e) SH-activated pastes; Cumulative heat of (b) SS-activated pastes, (d) SC-activated pastes, (f) SH-activated pastes (Teker Ercan et al. [91]).

5. Conclusions

The conclusions for research questions which were formulated for this part of the project are as follows:

1. How does the different wood ash grinding parameters affected on alkali-activated wood ash? **(Study A)**
   - Grinding of wood ash improved the compressive strength of the alkali-activated wood ash mortars. However, it was only a preliminary test. Grinding effect on the wood ash will be further investigated.

2. How does the pozzolanic activity of wood ash is affected by ball milling? **(Study C)**
   - Pozzolanic reactivity of wood ash increased by ball milling for both grinding durations.

3. How do different types of alkali-activators affect the mechanical properties of wood ash-containing alkali-activated mortars? **(Study D – Paper II)**
   - SS-activated samples showed the highest mechanical strength and 10 wt% of 10 minutes ground wood ash improved compressive strength compared to control sample. On the other hand, increasing wood ash ratio decreased the mechanical strength and increased the porosity.

4. How does the chemical composition of wood ash affect the properties of concrete?
   - The research was started and will be the focus in the second part.

5. How the effect of variability of properties of wood ashes originating from different sources on their reactivity (used as SCM and as precursor in alkali activated system) could be limited?
   - The research was started and will be the focus in the second part.

The results showed that ball milling has positive a promising effect on the wood ash and wood ash containing materials.

6. Future work

In the second phase of the PhD project, the focus will be on the following topics:

- Further investigation of enhancing the pozzolanic properties of different types of wood ashes through ball milling.
- Utilization of wood ash in cement-based materials and evaluation of their mechanical and durability properties.

References

1. Monteiro, P.J.M.; Miller, S.A.; Horvarth, A. Towards Sustainable Concrete. *Nat. Mater.* **2017**, *16*, 698–699, doi:https://doi.org/10.1038/nmat4930.
2. Teixeira, E.R.; Camões, A.; Branco, F.G. Valorisation of Wood Fly Ash on Concrete. *Resour. Conserv. Recycl.* **2019**, *145*, 292–310, doi:10.1016/j.resconrec.2019.02.028.
3. Teixeira, E.R.; Mateus, R.; Camões, A.F.; Bragança, L.; Branco, F.G. Comparative Environmental Life-Cycle Analysis of Concretes Using Biomass and Coal Fly Ashes as Partial Cement Replacement Material. *J. Clean. Prod.* **2016**, *112*, 2221–2230, doi:10.1016/J.JCLEPRO.2015.09.124.
4. Ukrainczyk, N.; Vrbos, N.; Koenders, E.A.B. Reuse of Woody Biomass Ash Waste in Cementitious Materials. *Chem. Biochem. Eng. Q.* **2016**, *30*, 137–148, doi:10.15255/CABEQ.2015.2231.
5. Bakhoum, E.S.; Amir, A.; Osama, F.; Adel, M. Prediction Model for the Compressive Strength of Green Concrete Using Cement Kiln Dust and Fly Ash. *Sci. Rep.* **2023**, *13*, doi:10.1038/s41598-023-28868-7.
6. Ramos, T.; Matos, A.M.; Sousa-Coutinho, J. Mortar with Wood Waste Ash: Mechanical Strength Carbonation Resistance and ASR Expansion. *Constr. Build. Mater.* **2013**, *49*, 343–351, doi:10.1016/j.conbuildmat.2013.08.026.
7. de Brito, J.; Kurda, R. The Past and Future of Sustainable Concrete: A Critical Review and New Strategies on Cement-Based Materials. *J. Clean. Prod.* **2021**, *281*, doi:10.1016/j.jclepro.2020.123558.
8. Tripathi, N.; Hills, C.D.; Singh, R.S.; Singh, J.S. Offsetting Anthropogenic Carbon Emissions from Biomass Waste and Mineralised Carbon Dioxide. *Sci. Rep.* **2020**, *10*, doi:10.1038/s41598-020-57801-5.
9. Global Cement and Concrete Association Https://Gccassociation.Org.
10. Hills, C.D.; Tripathi, N.; Singh, R.S.; Carey, P.J.; Lowry, F. Valorisation of Agricultural Biomass-Ash with CO2. *Sci. Rep.* **2020**, *10*, 13801, doi:10.1038/s41598-020-70504-1.
11. Lazik, P.-R.; Bošnjak, J.; Cetin, E.; Kücük, A. Application of Wood Ash as a Substitute For Fly Ash And Investigation of Concrete Properties. *Otto-Graf-Journal* **2020**, *19*.
12. Gerges, N.; Issa, C.A.; Antoun, M.; Sleiman, E.; Hallal, F.; Shamoun, P.; Hayek, J. Eco-Friendly Mortar: Optimum Combination of Wood Ash, Crumb Rubber, and Fine Crushed Glass. *Case Stud. Constr. Mater.* **2021**, *15*, doi:10.1016/j.cscm.2021.e00588.
13. Omran, A.; Soliman, N.; Xie, A.; Davidenko, T.; Tagnit-Hamou, A. Field Trials with Concrete Incorporating Biomass-Fly Ash. *Constr. Build. Mater.* **2018**, *186*, 660–669, doi:10.1016/j.conbuildmat.2018.07.084.
14. Siddique, R. Utilization of Wood Ash in Concrete Manufacturing. *Resour. Conserv. Recycl.* **2012**, *67*, 27–33, doi:10.1016/j.resconrec.2012.07.004.
15. Tripathi, N.; Hills, C.D.; Singh, R.S.; Atkinson, C.J. Biomass Waste Utilisation in Low-Carbon Products: Harnessing a Major Potential Resource. *npj Clim. Atmos. Sci.* **2019**, *2*, doi:10.1038/s41612-019-0093-5.
16. Etiégni, L.; Campbell, A.G. Physical and Chemical Characteristics of Wood Ash*. *Bioresour. Technol.* **1991**, *37*, 173–178.
17. Chowdhury, S.; Mishra, M.; Suganya, O. The Incorporation of Wood Waste Ash as a

Partial Cement Replacement Material for Making Structural Grade Concrete: An Overview. *Ain Shams Eng. J.* **2015**, *6*, 429–437, doi:10.1016/j.asej.2014.11.005.
18. James, A.K.; Thring, R.W.; Helle, S.; Ghuman, H.S. Ash Management Review-Applications of Biomass Bottom Ash. *Energies* **2012**, *5*, 3856–3873, doi:10.3390/en5103856.
19. Udoeyo, F.F.; Inyang, H.; David, Y.T.; Oparadu, E.E. Potential of Wood Waste Ash as an Additive in Concrete. *J. Mater. Civ. Eng.* **2006**, doi:10.1061/ASCE0899-1561200618:4605.
20. Sigvardsen, N.M.; Kirkelund, G.M.; Jensen, P.E.; Geiker, M.R.; Ottosen, L.M. Impact of Production Parameters on Physiochemical Characteristics of Wood Ash for Possible Utilisation in Cement-Based Materials. *Resour. Conserv. Recycl.* **2019**, *145*, 230–240, doi:10.1016/j.resconrec.2019.02.034.
21. Cheah, C.B.; Ramli, M. The Implementation of Wood Waste Ash as a Partial Cement Replacement Material in the Production of Structural Grade Concrete and Mortar: An Overview. *Resour. Conserv. Recycl.* **2011**, *55*, 669–685, doi:10.1016/j.resconrec.2011.02.002.
22. Maresca, A.; Hansen, M.; Ingerslev, M.; Astrup, T.F. Column Leaching from a Danish Forest Soil Amended with Wood Ashes: Fate of Major and Trace Elements. *Biomass and Bioenergy* **2018**, *109*, 91–99, doi:10.1016/J.BIOMBIOE.2017.12.014.
23. Berra, M.; Mangialardi, T.; Paolini, A.E. Reuse of Woody Biomass Fly Ash in Cement-Based Materials. *Constr. Build. Mater.* **2015**, *76*, 286–296, doi:10.1016/j.conbuildmat.2014.11.052.
24. Ottosen, L.M.; Hansen, E.Ø.; Jensen, P.E.; Kirkelund, G.M.; Golterman, P. Wood Ash Used as Partly Sand and/or Cement Replacement in Mortar. *Int. J. Sustain. Dev. Plan.* **2016**, *11*, 781–791, doi:10.2495/SDP-V11-N5-781-791.
25. EN 450-1 Fly Ash for Concrete - Part 1: Definition, Specifications and Conformity Criteria. **2012**, *50*.
26. ASTM C618-15; International, A.; indexed by mero, files Standard Specification for Coal Fly Ash and Raw or Calcined Natural Pozzolan for Use in Concrete. **2015**.
27. Abdullahi, M. Characteristics of Wood ASH/OPC Concrete. *Leonardo Electron. J. Pract. Technol.* **2006**, 9–16.
28. Carević, I.; Serdar, M.; Štirmer, N.; Ukrainczyk, N. Preliminary Screening of Wood Biomass Ashes for Partial Resources Replacements in Cementitious Materials. *J. Clean. Prod.* **2019**, *229*, 1045–1064, doi:10.1016/j.jclepro.2019.04.321.
29. Rajamma, R.; Ball, R.J.; Tarelho, L.A.C.; Allen, G.C.; Labrincha, J.A.; Ferreira, V.M. Characterisation and Use of Biomass Fly Ash in Cement-Based Materials. *J. Hazard. Mater.* **2009**, *172*, 1049–1060, doi:10.1016/j.jhazmat.2009.07.109.
30. Garcia, M.D.L.; Sousa-Coutinho, J. Strength and Durability of Cement with Forest Waste Bottom Ash. *Constr. Build. Mater.* **2013**, *41*, 897–910, doi:10.1016/j.conbuildmat.2012.11.081.
31. Vassilev, S. V.; Baxter, D.; Andersen, L.K.; Vassileva, C.G. An Overview of the Chemical Composition of Biomass. *Fuel* **2010**, *89*, 913–933, doi:10.1016/j.fuel.2009.10.022.
32. Carević, I.; Baričević, A.; Štirmer, N.; Šantek Bajto, J. Correlation between Physical

and Chemical Properties of Wood Biomass Ash and Cement Composites Performances. *Constr. Build. Mater.* **2020**, *256*, doi:10.1016/j.conbuildmat.2020.119450.
33. Sigvardsen, N.M.; Geiker, M.R.; Ottosen, L.M. Phase Development and Mechanical Response of Low-Level Cement Replacements with Wood Ash and Washed Wood Ash. *Constr. Build. Mater.* **2021**, *269*, 121234, doi:10.1016/J.CONBUILDMAT.2020.121234.
34. Elinwa, A.U.; Mahmood, Y.A. Ash from Timber Waste as Cement Replacement Material. *Cem. Concr. Compos.* **2002**, *24*, 219–222, doi:10.1016/S0958-9465(01)00039-7.
35. Ngueyep, M.; Leroy, L. Valorization of Wood Ashes as Partial Replacement of Portland Cement: Mechanical Performance and Durability. *Eur. J. Sci. Res.* **2019**, *151*, 468–478.
36. Chowdhury, S.; Maniar, A.; Suganya, O.M. Strength Development in Concrete with Wood Ash Blended Cement and Use of Soft Computing Models to Predict Strength Parameters. *J. Adv. Res.* **2015**, *6*, 907–913, doi:10.1016/j.jare.2014.08.006.
37. ASTM C311/C311M-13; ASTM C311 Standard Test Methods for Sampling and Testing Fly Ash or Natural Pozzolans for Use in Portland-Cement Concrete. **2007**.
38. EN 196-2 Method of Testing Cement – Part 2: Chemical Analysis of Cement. **2013**.
39. Hamid, Z.; Rafiq, S. A Comparative Study on Strength of Concrete Using Wood Ash as Partial Replacement of Cement. In Proceedings of the IOP Conference Series: Materials Science and Engineering; IOP Publishing Ltd, November 20 2020; Vol. 955.
40. Doudart de la Grée, G.C.H.; Florea, M.V.A.; Keulen, A.; Brouwers, H.J.H. Contaminated Biomass Fly Ashes - Characterization and Treatment Optimization for Reuse as Building Materials. *Waste Manag.* **2016**, *49*, 96–109, doi:10.1016/j.wasman.2015.12.023.
41. Amaral, R.C.; Rohden, A.B.; Garcez, M.R.; Andrade, J.J. de O. Reuse of Wood Ash from Biomass Combustion in Non-structural Concrete: Mechanical Properties, Durability, and Eco-efficiency. *J. Mater. Cycles Waste Manag. Vol.* **2022**, *24*, 2439–2454.
42. Massazza, F. Pozzolana and Pozzolanic Cements. In *Lea's Chemistry of Cement and Concrete*; Elsevier, 1998; pp. 471–635.
43. Jurić, K.K.; Carević, I.; Serdar, M.; Štirmer, N. Feasibility of Using Pozzolanicity Tests to Assess Reactivity of Wood Biomass Fly Ashes. *Gradjevinar* **2021**, *72*, 1145–1153, doi:10.14256/JCE.2950.2020.
44. Fořt, J.; Šál, J.; Žák, J.; Černý, R. Assessment of Wood-Based Fly Ash as Alternative Cement Replacement. *Sustain.* **2020**, *12*, 1–16, doi:10.3390/su12229580.
45. Demis, S.; Tapali, J.G.; Papadakis, V.G. An Investigation of the Effectiveness of the Utilization of Biomass Ashes as Pozzolanic Materials. *Constr. Build. Mater.* **2014**, *68*, 291–300, doi:10.1016/J.CONBUILDMAT.2014.06.071.
46. Snellings, R.; Mertens, G.; Elsen, J. Supplementary Cementitious Materials. *Rev. Mineral. Geochemistry* **2012**, *74*, 211–278, doi:10.2138/rmg.2012.74.6.
47. EN 197-1 Cement – Part 1 : Composition, Specifications and Conformity Criteria for Common Cements. **2011**.
48. Ban, C.C.; Ken, P.W.; Ramli, M. Mechanical and Durability Performance of Novel Self-Activating Geopolymer Mortars. In Proceedings of the Procedia Engineering; Elsevier Ltd, 2017; Vol. 171, pp. 564–571.

49. Carević, I.; Pečur, I.B.; Štirmer, N. Durability Properties of Cement Composities with Wood Biomass Ash. In Proceedings of the 4th International Conference of Service Life Design for Infrastructures (SLD4), 27-30 August 2018, RILEM WEEK 2018 At: Delft, Netherlands; 2018.
50. Sharma, M.; Lalotra, S. An Experimental Study on Strength of Concrete with Partial Replacement of Cement by Wood Ash and Fine Aggregate by Copper Slag. *Int. Res. J. Eng. Technol.* **2022**, *9*, 412–418.
51. Rajamma, R.; Senff, L.; Ribeiro, M.J.; Labrincha, J.A.; Ball, R.J.; Allen, G.C.; Ferreira, V.M. Biomass Fly Ash Effect on Fresh and Hardened State Properties of Cement Based Materials. *Compos. Part B Eng.* **2015**, *77*, 1–9, doi:10.1016/j.compositesb.2015.03.019.
52. Brazão Farinha, C.; de Brito, J.; Veiga, R. Influence of Forest Biomass Bottom Ashes on the Fresh, Water and Mechanical Behaviour of Cement-Based Mortars. *Resour. Conserv. Recycl.* **2019**, *149*, 750–759, doi:10.1016/J.RESCONREC.2019.06.020.
53. Yang, Z.; Huddleston, J.; Brown, H. Effects of Wood Ash on Properties of Concrete and Flowable Fill. *J. Mater. Sci. Chem. Eng.* **2016**, *04*, 101–114, doi:10.4236/msce.2016.47013.
54. Elinwa, A.U.; Ejeh, S.P. Effects of the Incorporation of Sawdust Waste Incineration Fly Ash in Cement Pastes and Mortars. *J. Asian Archit. Build. Eng.* **2004**, *3*, 1–7, doi:10.3130/JAABE.3.1.
55. Chen, H.J.; Shih, N.H.; Wu, C.H.; Lin, S.K. Effects of the Loss on Ignition of Fly Ash on the Properties of High-Volume Fly Ash Concrete. *Sustain.* **2019**, *11*, doi:10.3390/su11092704.
56. Sklivaniti, V.; Tsakiridis, P.E.; Katsiotis, N.S.; Velissariou, D.; Pistofidis, N.; Papageorgiou, D.; Beazi, M. Valorisation of Woody Biomass Bottom Ash in Portland Cement: A Characterization and Hydration Study. *J. Environ. Chem. Eng.* **2017**, *5*, 205–213, doi:10.1016/j.jece.2016.11.042.
57. Subramaniam, P.; Subasinghe, K.; Fonseka, W.R.K. Wood Ash as An Effective Raw Material for Concrete Blocks. In Proceedings of the IJRET: International Journal of Research in Engineering and Technology; February 2015; pp. 228–233.
58. Naik, T.R.; Kraus, R.N.; Siddique, R. Demonstration of Manufacturing Technology for Concrete and CLSM Utilizing Wood Ash from Wisconsin. *UWM Cent. By Prod. Util.* **2002**, *538*, 124.
59. Udoeyo, F.F.; Dashibil, P.U. Sawdust Ash as Concrete Material. *J. Mater. Civ. Eng.* **2002**, *14*, 173–176.
60. Lessard, J.-M.; Omran, A.; Tagnit-Hamou, A.; Gagne, R. Feasibility of Using Biomass Fly and Bottom Ashes to Produce RCC and PCC. *J. Mater. Civ. Eng.* **2017**, *29*, 04016267, doi:10.1061/(asce)mt.1943-5533.0001796.
61. Raju, R.; Paul, M.M.; Aboobacker, K.A. Strength Performance of Concrete Using Bottom Ash as Fine Aggregate. *Impact Journals* **2014**, *2*, 111–122.
62. Candamano, S.; Crea, F.; Romano, D.; Iacobini, I. Workability, Strength and Drying Shrinkage of Structural Mortar Containing Forest Biomass Ash in Partial Replacement of Cement. In Proceedings of the Advanced Materials Research; Trans Tech Publications Ltd, 2014; Vol. 1051, pp. 73–742.
63. Cheah, C.B.; Ramli, M. The Engineering Properties of High Performance Concrete

with HCWA-DSF Supplementary Binder. *Constr. Build. Mater.* **2013**, *40*, 93–103, doi:10.1016/j.conbuildmat.2012.10.010.
64. Cheah, C.B.; Ramli, M. Mechanical Strength, Durability and Drying Shrinkage of Structural Mortar Containing HCWA as Partial Replacement of Cement. *Constr. Build. Mater.* **2012**, *30*, 320–329, doi:10.1016/j.conbuildmat.2011.12.009.
65. Rissanen, J.; Ohenoja, K.; Kinnunen, P.; Illikainen, M. Peat-Wood Fly Ash as Cold-Region Supplementary Cementitious Material: Air Content and Freeze-Thaw Resistance of Air-Entrained Mortars. **2020**, doi:10.1061/(ASCE)MT.1943.
66. Kothari, A.; Habermehl-Cwirzen, K.; Hedlund, H.; Cwirzen, A. A Review of the Mechanical Properties and Durability of Ecological Concretes in a Cold Climate in Comparison to Standard Ordinary Portland Cement-Based Concrete. *Materials (Basel).* **2020**, *13*, doi:10.3390/MA13163467.
67. Wang, S.; Llamazos, E.; Baxter, L.; Fonseca, F. Durability of Biomass Fly Ash Concrete: Freezing and Thawing and Rapid Chloride Permeability Tests. *Fuel* **2008**, *87*, 359–364, doi:10.1016/j.fuel.2007.05.027.
68. Kandasamy, S.; Shehata, M.H. The Capacity of Ternary Blends Containing Slag and High-Calcium Fly Ash to Mitigate Alkali Silica Reaction. *Cem. Concr. Compos.* **2014**, *49*, 92–99, doi:10.1016/J.CEMCONCOMP.2013.12.008.
69. Ramyar, K.; Çopuroğlu, O.; Andiç, Ö.; Fraaij, A.L.A. Comparison of Alkali–silica Reaction Products of Fly-Ash- or Lithium-Salt-Bearing Mortar under Long-Term Accelerated Curing. *Cem. Concr. Res.* **2004**, *34*, 1179–1183, doi:10.1016/J.CEMCONRES.2003.12.007.
70. Esteves, T.C.; Rajamma, R.; Soares, D.; Silva, A.S.; Ferreira, V.M.; Labrincha, J.A. Use of Biomass Fly Ash for Mitigation of Alkali-Silica Reaction of Cement Mortars. *Constr. Build. Mater.* **2012**, *26*, 687–693, doi:10.1016/j.conbuildmat.2011.06.075.
71. ASTM C33/C33M-18 Standard Specification for Concrete Aggregates. **2018**.
72. Provis, J.L. Geopolymers and Other Alkali Activated Materials: Why, How, and What? *Mater. Struct. Constr.* **2014**, *47*, 11–25, doi:10.1617/s11527-013-0211-5.
73. Luukkonen, T.; Abdollahnejad, Z.; Yliniemi, J.; Kinnunen, P.; Illikainen, M. One-Part Alkali-Activated Materials: A Review. *Cem. Concr. Res.* **2018**, *103*, 21–34, doi:10.1016/J.CEMCONRES.2017.10.001.
74. Şanal, İ. Significance of Concrete Production in Terms of Carbondioxide Emissions: Social and Environmental Impacts. *J. Polytech.* **2018**, *0900*, 369–378, doi:10.2339/politeknik.389590.
75. Flower, D.J.M.; Sanjayan, J.G. Greenhouse Gas Emissions Due to Concrete Manufacture. *Handb. Low Carbon Concr.* **2017**, *12*, 1–16, doi:10.1016/B978-0-12-804524-4.00001-4.
76. Humad, A.M.; Habermehl-Cwirzen, K.; Cwirzen, A. Effects of Fineness and Chemical Composition of Blast Furnace Slag on Properties of Alkali-Activated Binder. *Materials (Basel).* **2019**, *12*, 1–16, doi:10.3390/ma12203447.
77. Long, H.V. Optimizing Mixtures of Alkali Aluminosilicate Cement Based on Ternary By-Products. *Civ. Eng. J.* **2021**, *7*, 1264–1274, doi:10.28991/cej-2021-03091724.
78. Jiang, M.; Chen, X.; Rajabipour, F.; Hendrickson, C.T. Comparative Life Cycle Assessment of Conventional, Glass Powder, and Alkali-Activated Slag Concrete and

Mortar. *J. Infrastruct. Syst.* **2014**, *20*, 1–9, doi:10.1061/(asce)is.1943-555x.0000211.
79. Awoyera, P.O.; Adesina, A.; Sivakrishna, A.; Gobinath, R.; Kumar, K.R.; Srinivas, A. Alkali Activated Binders: Challenges and Opportunities. In Proceedings of the Materials Today: Proceedings; Elsevier Ltd, January 1 2020; Vol. 27, pp. 40–43.
80. Puertas, F.; González-Fonteboa, B.; González-Taboada, I.; Alonso, M.M.; Torres-Carrasco, M.; Rojo, G.; Martínez-Abella, F. Alkali-Activated Slag Concrete: Fresh and Hardened Behaviour. *Cem. Concr. Compos.* **2018**, *85*, 22–31, doi:10.1016/j.cemconcomp.2017.10.003.
81. Owaid, H.M.; Al-Rubaye, M.M.; Al-Baghdadi, H.M. Use of Waste Paper Ash or Wood Ash as Substitution to Fly Ash in Production of Geopolymer Concrete. *Sci. Rev. Eng. Environ. Sci.* **2021**, *30*, 464–476, doi:10.22630/PNIKS.2021.30.3.39.
82. Cheah, C.B.; Part, W.K.; Ramli, M. The Hybridizations of Coal Fly Ash and Wood Ash for the Fabrication of Low Alkalinity Geopolymer Load Bearing Block Cured at Ambient Temperature. *Constr. Build. Mater.* **2015**, *88*, 41–55, doi:10.1016/j.conbuildmat.2015.04.020.
83. Samsudin, M.H.; Chee Ban, C. Granulated Blast Furnace Slag and High Calcium Wood Ash (GGBS-HCWA) for the Fabrication of Geopolymer Mortar. *Adv. Environ. Biol.* **2015**, *9*, 22–25.
84. Abdulkareem, O.A.; Ramli, M.; Matthews, J.C. Production of Geopolymer Mortar System Containing High Calcium Biomass Wood Ash as a Partial Substitution to Fly Ash: An Early Age Evaluation. *Compos. Part B Eng.* **2019**, *174*, 106941, doi:10.1016/j.compositesb.2019.106941.
85. Cheah, C.B.; Part, W.K.; Ramli, M. The Long Term Engineering Properties of Cementless Building Block Work Containing Large Volume of Wood Ash and Coal Fly Ash. *Constr. Build. Mater.* **2017**, *143*, 522–536, doi:10.1016/j.conbuildmat.2017.03.162.
86. Candamano, S.; De Luca, P.; Frontera, P.; Crea, F. Production of Geopolymeric Mortars Containing Forest Biomass Ash as Partial Replacement of Metakaolin. *Environ. - MDPI* **2017**, *4*, 1–13, doi:10.3390/environments4040074.
87. De Rossi, A.; Simão, L.; Ribeiro, M.J.; Hotza, D.; Moreira, R.F.P.M. Study of Cure Conditions Effect on the Properties of Wood Biomass Fly Ash Geopolymers. *J. Mater. Res. Technol.* **2020**, *9*, 7518–7528, doi:10.1016/j.jmrt.2020.05.047.
88. Silva, G.J.B.; Santana, V.P.; Wójcik, M. Investigation on Mechanical and Microstructural Properties of Alkali-Activated Materials Made of Wood Biomass Ash and Glass Powder. *Powder Technol.* **2021**, *377*, 900–912, doi:10.1016/j.powtec.2020.09.048.
89. Bajare, D.; Bumanis, G.; Shakhmenko, G.; Justs, J. Obtaining Composition of Geopolymers (Alkali Activated Binders) from Local Industrial Wastes. In Proceedings of the 3rd International Conference CIVIL ENGINEERING`11 Proceedings ; 2011; pp. 50–56.
90. Ates, F.; Park, K.T.; Kim, K.W.; Woo, B.-H.; Kim, H.G. Effects of Treated Biomass Wood Fly Ash as a Partial Substitute for Fly Ash in a Geopolymer Mortar System. *Constr. Build. Mater.* **2023**, *376*, 131063, doi:10.1016/j.conbuildmat.2023.131063.
91. Teker Ercan, E.E.; Cwirzen, A.; Habermehl-Cwirzen, K. The Effects of Partial

Replacement of Ground Granulated Blast Furnace Slag by Ground Wood Ash on Alkali-Activated Binder Systems. *Materials (Basel).* **2023**, *16*, 5347.
92. Tole, I.; Rajczakowska, M.; Humad, A.; Kothari, A.; Cwirzen, A. Geopolymer Based on Mechanically Activated Air-Cooled Blast Furnace Slag. *Materials (Basel).* **2020**, *13*, doi:10.3390/ma13051134.
93. Aydin, S.; Baradan, B. Effect of Activator Type and Content on Properties of Alkali-Activated Slag Mortars. *Compos. Part B Eng.* **2014**, *57*, 166–172, doi:10.1016/j.compositesb.2013.10.001.
94. Li, Y.; Sun, Y. Preliminary Study on Combined-Alkali-Slag Paste Materials. *Cem. Concr. Res.* **2000**, *30*, 963–966, doi:10.1016/S0008-8846(00)00269-6.
95. Chang, J.J. A Study on the Setting Characteristics of Sodium Silicate-Activated Slag Pastes. *Cem. Concr. Res.* **2003**, *33*, 1005–1011, doi:10.1016/S0008-8846(02)01096-7.
96. Kirkelund, G.M.; Ottosen, L.M.; Jensen, P.E.; Goltermann, P. Greenlandic Waste Incineration Fly and Bottom Ash as Secondary Resource in Mortar. *Int. J. Sustain. Dev. Plan.* **2016**, *11*, 719–728, doi:10.2495/SDP-V11-N5-719-728.
97. BS EN 196 - 1 Methods of Testing Cement. *Part 1 Determ. strength* **2005**, *BS EN 169-*, 36.
98. EN 196-5 Methods of Testing Cement - Part 5 - Pozzolanicity Test for Pozzolanic Cement. **2011**.
99. Tole, I.; Delogu, F.; Qoku, E.; Habermehl-Cwirzen, K.; Cwirzen, A. Enhancement of the Pozzolanic Activity of Natural Clays by Mechanochemical Activation. *Constr. Build. Mater.* **2022**, *352*, 128739, doi:10.1016/j.conbuildmat.2022.128739.
100. Donatello, S.; Tyrer, M.; Cheeseman, C.R. Comparison of Test Methods to Assess Pozzolanic Activity. *Cem. Concr. Compos.* **2010**, *32*, 121–127, doi:10.1016/j.cemconcomp.2009.10.008.
101. Tironi, A.; Trezza, M.A.; Scian, A.N.; Irassar, E.F. Assessment of Pozzolanic Activity of Different Calcined Clays. *Cem. Concr. Compos.* **2013**, *37*, 319–327, doi:10.1016/j.cemconcomp.2013.01.002.
102. Rossen, J.E.; Scrivener, K.L. Optimization of SEM-EDS to Determine the C–A–S–H Composition in Matured Cement Paste Samples. *Mater. Charact.* **2017**, *123*, 294–306, doi:10.1016/j.matchar.2016.11.041.
103. Scrivener, K.L. Backscattered Electron Imaging of Cementitious Microstructures: Understanding and Quantification. *Cem. Concr. Compos.* **2004**, *26*, 935–945, doi:10.1016/j.cemconcomp.2004.02.029.
104. ASTM C1702-17 Standard Test Method for Measurement of Heat of Hydration of Hydraulic Cementitious Materials Using Isothermal Conduction Calorimetry. *ASTM Int.* **2017**.
105. Ikumapayi, O.M.; Akinlabi, E.T.; Adedeji, P.A.; Akinlabi, S.A. Comparative Analysis of Milling Time on the Particle Sizes of Coal Fly Ash and Wood Fly Ash Using Otsu Method for Thresholding. *J. Phys. Conf. Ser.* **2019**, *1378*, doi:10.1088/1742-6596/1378/4/042075.
106. Hamzaoui, R.; Bouchenafa, O.; Guessasma, S.; Leklou, N.; Bouaziz, A. The Sequel of Modified Fly Ashes Using High Energy Ball Milling on Mechanical Performance of Substituted Past Cement. *Mater. Des.* **2016**, *90*, 29–37,

doi:10.1016/J.MATDES.2015.10.109.
107. Kumar, S.; Kumar, R. Mechanical Activation of Fly Ash: Effect on Reaction, Structure and Properties of Resulting Geopolymer. *Ceram. Int.* **2011**, *37*, 533–541, doi:10.1016/j.ceramint.2010.09.038.
108. Rissanen, J.; Ohenoja, K.; Kinnunen, P.; Romagnoli, M.; Illikainen, M. Milling of Peat-Wood Fly Ash: Effect on Water Demand of Mortar and Rheology of Cement Paste. *Constr. Build. Mater.* **2018**, *180*, 143–153, doi:10.1016/J.CONBUILDMAT.2018.05.014.
109. Peng, Y. xing; Ni, X.; Zhu, Z. cai; Yu, Z. fa; Yin, Z. xin; Li, T. qing; Liu, S. yong; Zhao, L. la; Xu, J. Friction and Wear of Liner and Grinding Ball in Iron Ore Ball Mill. *Tribol. Int.* **2017**, *115*, 506–517, doi:10.1016/j.triboint.2017.06.017.
110. Silvestro, L.; Scolaro, T.P.; Ruviaro, A.S.; Santos Lima, G.T. dos; Gleize, P.J.P.; Pelisser, F. Use of Biomass Wood Ash to Produce Sustainable Geopolymeric Pastes. *Constr. Build. Mater.* **2023**, *370*, doi:10.1016/j.conbuildmat.2023.130641.
111. Silva, T.H.; Lara, L.F.S.; Silva, G.J.B.; Provis, J.L.; Bezerra, A.C.S. Alkali-Activated Materials Produced Using High-Calcium, High-Carbon Biomass Ash. *Cem. Concr. Compos.* **2022**, *132*, doi:10.1016/j.cemconcomp.2022.104646.
112. Senneca, O.; Salatino, P.; Chirone, R.; Cortese, L.; Solimene, R. Mechanochemical Activation of High-Carbon Fly Ash for Enhanced Carbon Reburning. *Proc. Combust. Inst.* **2011**, *33*, 2743–2753, doi:10.1016/j.proci.2010.07.067.
113. Marjanović, N.; Komljenović, M.; Baščarević, Z.; Nikolić, V. Improving Reactivity of Fly Ash and Properties of Ensuing Geopolymers through Mechanical Activation. *Constr. Build. Mater.* **2014**, *57*, 151–162, doi:10.1016/j.conbuildmat.2014.01.095.
114. Aydin, S.; Karatay, Ç.; Baradan, B. The Effect of Grinding Process on Mechanical Properties and Alkali-Silica Reaction Resistance of Fly Ash Incorporated Cement Mortars. *Powder Technol.* **2010**, *197*, 68–72, doi:10.1016/j.powtec.2009.08.020.
115. Cheah, C.B.; Samsudin, M.H.; Ramli, M.; Part, W.K.; Tan, L.E. The Use of High Calcium Wood Ash in the Preparation of Ground Granulated Blast Furnace Slag and Pulverized Fly Ash Geopolymers: A Complete Microstructural and Mechanical Characterization. *J. Clean. Prod.* **2017**, *156*, 114–123, doi:10.1016/J.JCLEPRO.2017.04.026.
116. Dai, X.; Aydin, S.; Yardimci, M.Y.; De Schutter, G. Early Structural Build-up, Setting Behavior, Reaction Kinetics and Microstructure of Sodium Silicate-Activated Slag Mixtures with Different Retarder Chemicals. *Cem. Concr. Res.* **2022**, *159*, 106872, doi:10.1016/j.cemconres.2022.106872.
117. Fu, Q.; Bu, M.; Zhang, Z.; Xu, W.; Yuan, Q.; Niu, D. Hydration Characteristics and Microstructure of Alkali-Activated Slag Concrete: A Review. *Engineering* **2022**, *20*, 162–179, doi:10.1016/j.eng.2021.07.026.
118. Hu, X.; Shi, C.; Shi, Z.; Zhang, L. Compressive Strength, Pore Structure and Chloride Transport Properties of Alkali-Activated Slag/Fly Ash Mortars. *Cem. Concr. Compos.* **2019**, *104*, 103392, doi:10.1016/j.cemconcomp.2019.103392.
119. Cao, R.; Zhang, S.; Banthia, N.; Zhang, Y.; Zhang, Z. Interpreting the Early-Age Reaction Process of Alkali-Activated Slag by Using Combined Embedded Ultrasonic Measurement, Thermal Analysis, XRD, FTIR and SEM. *Compos. Part B Eng.* **2020**, *186*, 107840, doi:10.1016/j.compositesb.2020.107840.

120. Dai, X.; Ren, Q.; Aydin, S.; Yardimci, M.Y.; De Schutter, G. Accelerating the Reaction Process of Sodium Carbonate-Activated Slag Mixtures with the Incorporation of a Small Addition of Sodium Hydroxide/Sodium Silicate. *Cem. Concr. Compos.* **2023**, *141*, 105118, doi:10.1016/j.cemconcomp.2023.105118.
121. Wang, S.D.; Scrivener, K.L. Hydration Products of Alkali Activated Slag Cement. *Cem. Concr. Res.* **1995**, *25*, 561–571, doi:10.1016/0008-8846(95)00045-E.
122. Scrivener, K.; Ouzia, A.; Juilland, P.; Kunhi Mohamed, A. Advances in Understanding Cement Hydration Mechanisms. *Cem. Concr. Res.* **2019**, *124*, 105823, doi:10.1016/j.cemconres.2019.105823.
123. Provis, J.L.; van Deventer, J.S.J. *Alkali Materials Activated State-of-the-Art Report*; 2014; Vol. 13; ISBN 978-94-007-7671-5.
124. Dai, X.; Aydin, S.; Yardimci, M.Y.; Lesage, K.; de Schutter, G. Influence of Water to Binder Ratio on the Rheology and Structural Build-up of Alkali-Activated Slag/Fly Ash Mixtures. *Constr. Build. Mater.* **2020**, *264*, 120253, doi:10.1016/j.conbuildmat.2020.120253.
125. Bílek, V.; Kalina, L.; Novotný, R. Structural Build-up and Breakdown of Alkali-Activated Slag Pastes with Different Order of Lignosulfonate and Activator Addition. *Constr. Build. Mater.* **2023**, *386*, doi:10.1016/j.conbuildmat.2023.131557.

Department of Civil, Environmental and Natural Resources Engineering

---

Luleå University of Technology 2023